COMPUTATIONAL INVESTIGATION OF FLOW FIELD IN A CENTRIFUGAL SLURRY PUMP

Thesis submitted in partial fulfillment of the requirements for the award of degree of

Master of Engineering

In

CAD/CAM & ROBOTICS

By:
Rakesh Joshi
(800881019)

Under the supervision of:

Dr. S.K. Mohapatra
Professor & Head, MED

Mr. Satish Kumar
Assistant Professor, MED

MECHANICAL ENGINEERING DEPARTMENT
THAPAR UNIVERSITY
PATIALA – 147004

DECLARATION

I hereby declare that the work which is being presented in the dissertation work entitled, "**COMPUTATIONAL INVESTIGATION OF FLUID FIELD IN CENTRIFUGAL SLURRY PUMP**", in partial fulfillment of the requirements for the award of degree of Master of Engineering in Mechanical Engineering with specialization in **CAD/CAM & ROBOTICS** submitted in Mechanical Engineering Department of Thapar University, Patiala, is an authentic record of my own work carried out under the supervision of **Dr. S.K Mohapatra and Mr. Satish Kumar** refers other researcher's works which are duly listed in the reference section.

The matter presented in this thesis has not been submitted for the award of any other degree of this or any other university.

Date: - 15 July'2010
Place: - Patiala

Joshi
(RAKESH JOSHI)

.....

This is to certify that the above statement made by the candidate is correct and true to the best of my knowledge.

Supervisor:

Dr .S.K Mohapatra
Professor & Head
Mechanical Engineering Department
Thapar University, Patiala

Mr. Satish Kumar
Assistant Professor
Mechanical Engineering Department
Thapar University, Patiala

Dr. S.K Mohapatra
15/7/10
Professor & Head
Mechanical Engineering Department
University, Patiala

Dr. R.K. Sharma
29.7.10
Dean of Academic Affairs
Thapar University, Patiala Thapar

ACKNOWLEDGEMENT

like to express my most sincere appreciation and deep sense of gratitude and ess to my guides **Dr. S.K. Mohapatra** Professor and **Mr. Satish Kumar** Assistant Mechanical Engineering Department, Thapar University, Patiala for their continuous able guidance, which paved me on to the path to carry this project. I am highly indebted or their painstaking efforts and invaluable suggestions during the period of work.

uly'15

atiala

(Rakesh Joshi)

ABSTRACT

The choice of pumps or pumping systems for slurry transport will depend not only on the flow, head required, suction conditions, type of installation and location, as for any other pump application, but also on the slurry flow regime and properties. Centrifugal pump radial-flow type is the most common in slurry service. A conventional centrifugal pump is designed to handle clear liquids. However when slurries are to be transported the conventional centrifugal pump has to be modified to handle solid liquid mixtures. The modifications incorporated in the pump include enlargement of flow passages to accommodate bigger solid particles, robust impeller with smaller number of vanes, special seals and proper material of construction to ensure longer life. Conventional design method of centrifugal pump are largely based on the application of empirical and semi-empirical rules along with the use of available information in the form of different types of charts and graphs as proposed by successful designers. As the design of centrifugal pump involve a large number of interdependent variables, several other alternative design are possible for same duty. Computational fluid dynamics (CFD) is being increasingly applied in the design of the centrifugal pumps. 3-D numerical computational fluid dynamics tool can be used for simulation of the flow field characteristics inside the turbo machinery. Numerical simulation makes it possible to visualize the flow condition inside a centrifugal pump, and provides the valuable hydraulic design information of the centrifugal pumps. Present work is aimed to analyze the pressure and velocity distribution inside the pump passage and evaluate the pump performance using the Fluent, a computational fluid dynamics simulation tool. A numerical model of an impeller and casing has been generated and the complex internal pressure and velocity distribution are investigated by using the fluent computational code. . Pressure and velocity distribution inside impeller of the centrifugal pump has direct influence due to change of stream wise location.

CONTENTS

List of figures and tables

Nomenclature

D	Diameter, m
Q	Mass flow rate, m^3/sec
H	Head, m
N	Speed, RPM
ρ	Density of liquid, kg/m^3
$\vec{v}$	Velocity vector
$\bar{\bar{\tau}}$	Stress tensor
g	Acceleration due to gravity, m^2/sec
h_0	Enthalpy
μ_t	eddy viscosity
$\vec{F}$	Force vector, N
E	Total energy, J
$\dot{m}$	Flow rate
Q	flow rate of enthalpy, W
h	Species enthalpy
k	kinetic energy per unit mass, J/kg
U	Free stream velocity, m/s

Suffix:

i	x coordinate
j	y coordinate
z	z coordinate
1	inner diameter
2	outer diameter

CHAPTER -1

INTRODUCTION

1.1 PUMP

Pump is a device used to move fluids, such as liquids or slurries, or gases. Pump displaces a volume by physical or mechanical action .Or the hydraulic machine which converts mechanical energy into hydraulic energy is known as pump,

1.1.1 Classification of Pump

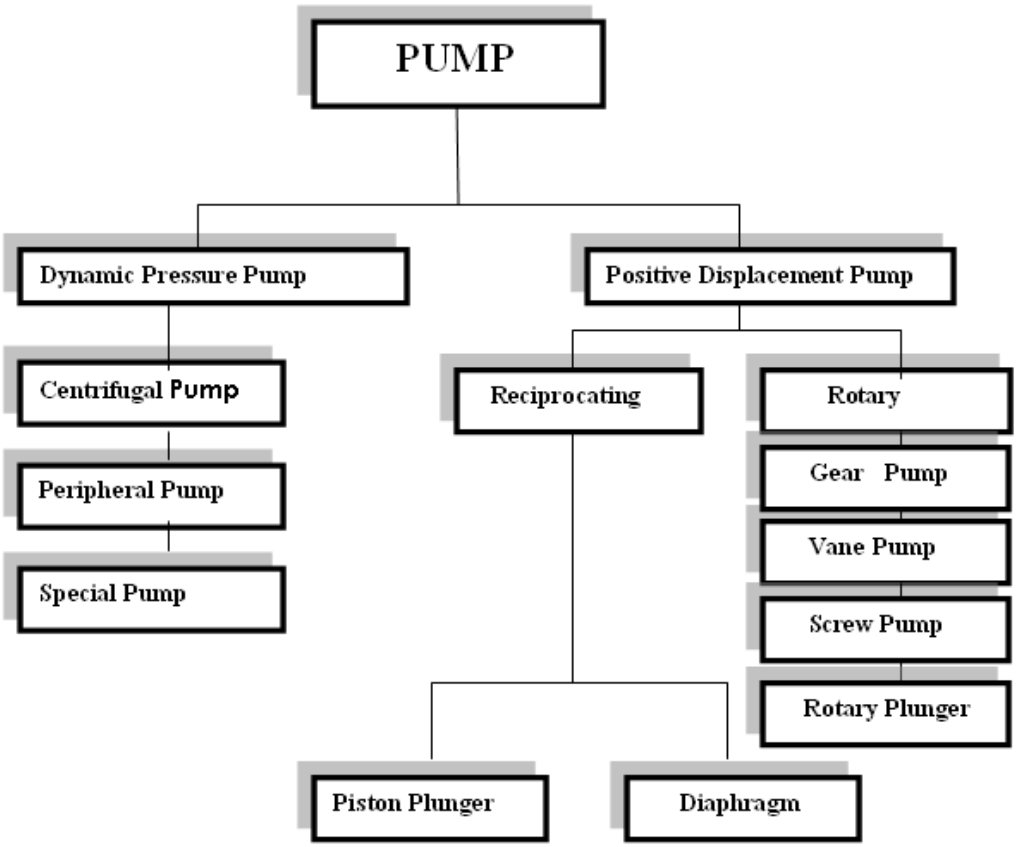

Figure 1.1: Classification of the pump

Reciprocating Pump:

Reciprocating pump is positive displacement pump in which mechanical energy is converted into hydraulic energy by sucking the liquid into a cylinder in which piston is reciprocating .This piston exert the thrust on the liquid and increases its pressure and hydraulic energy.

According to the water being in contact with piston ,the reciprocating pump are of two types named as single acting and double acting

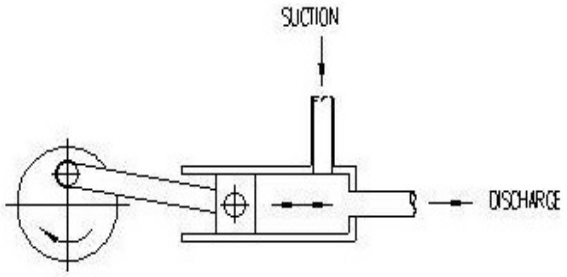

Figure 1.2 Reciprocating pump

Rotary pump:

Rotary pump is used to move heavy or very viscous fluids. These employ mechanical Means such as gear, cam and screw to move the liquid

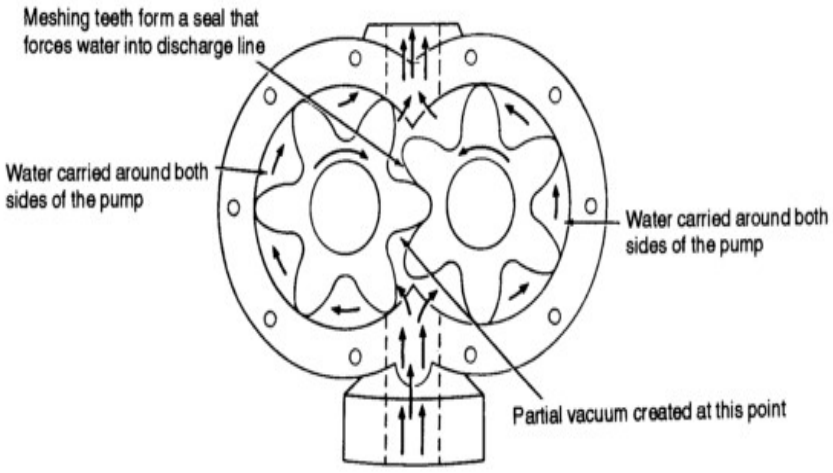

Figure 1.3: Sectional view of rotary pump

Centrifugal Pump:

Centrifugal pump is a pump in which mechanical energy is converted into pressure energy by means of centrifugal force acting on the fluid. It is classified as rotor dynamic type of pump in which dynamic pressure is developed which enables the lifting of liquids from lower level to higher level. Since in these pumps the lifting of liquid is due to centrifugal action that is why we called it as centrifugal pump. Centrifugal pump have high output and high effiency

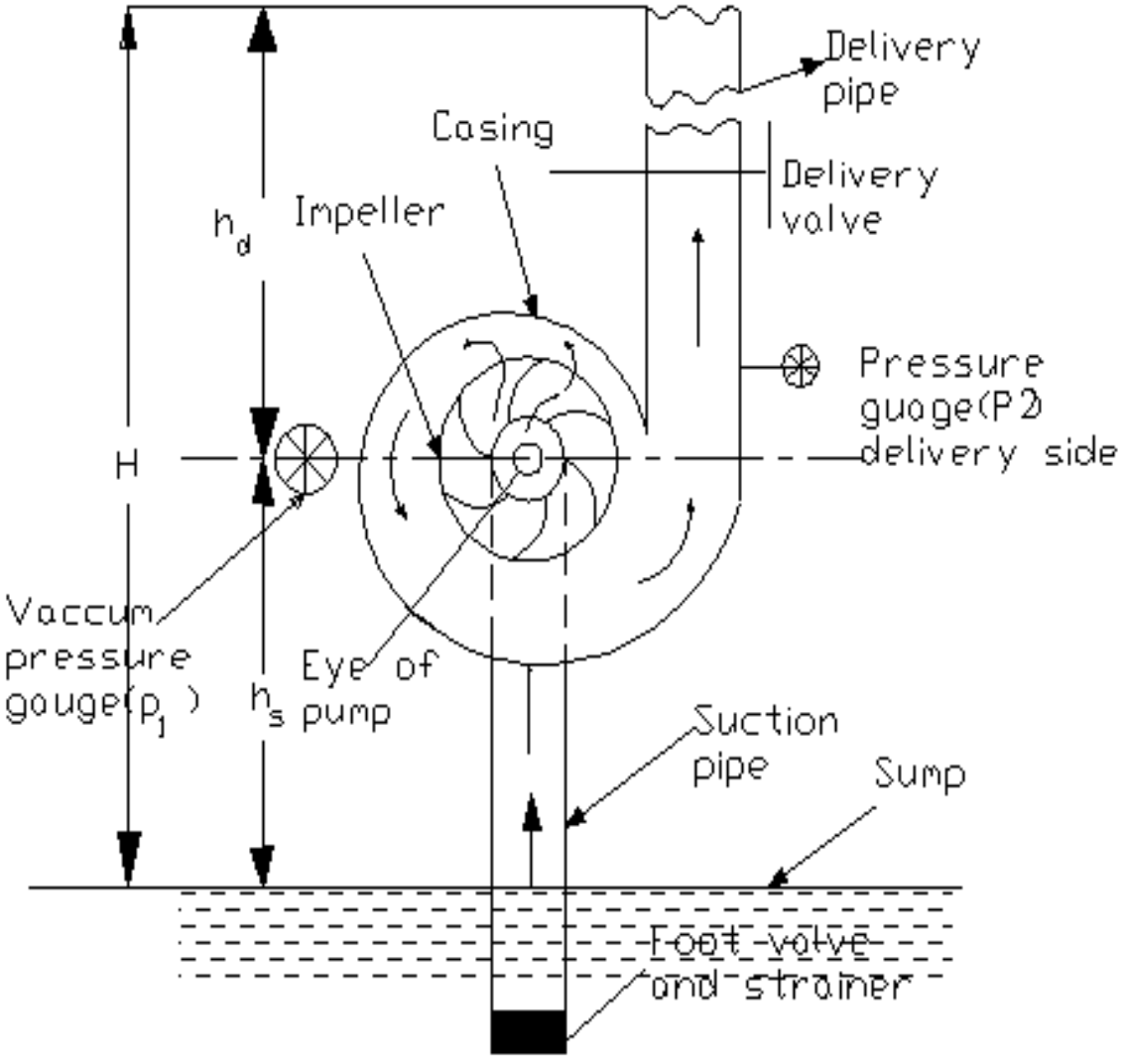

Figure 1.4 Centrifugal pump

1.2 WORKING PRINCIPLE OF CENTRIFUGAL PUMP

The centrifugal pump works on the principle of forced vortex flow .Which means that when a certain mass of liquid is rotated by an external flow, the rise in pressure head of the rotating liquid takes place. The rise in pressure head at any point of the rotating liquid is proportional to the square of the tangential velocity of the liquid at that point Thus at the outlet of the impeller where the radius is more, the rise in pressure head will be more and the liquid will be discharged at the outlet with high pressure head. Due to high-pressure head the liquid can lifted to high Level Figure 1.5 shows flow of fluid in a centrifugal pump.

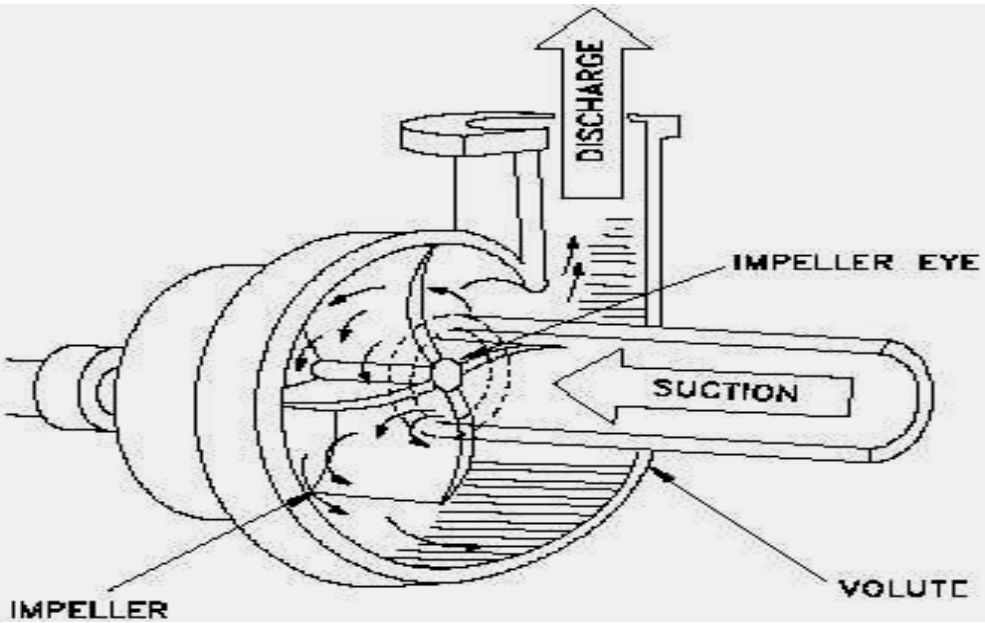

Figure 1.5 Flow of fluid in a centrifugal pump

1.2.1 Components of Centrifugal Pump

A centrifugal pump consists of flowing main components**;**

- Impeller
- Casing
- Suction pipe with a foot valve and a strainer
- Delivery Pipe

Impeller:

The rotating part of a centrifugal pump is called impeller .it consists of series of backward curved vanes. The impeller is mounted on a shaft coupled to driving unit which may be IC engine or an electric motor.

Casing:

Casing of a pump is an airtight passage surrounding the impeller and is consists suction and discharge arrangement, supporting for bearing and facilitate to house the rotor assembly. It is designed in such a way that the kinetic energy of water discharged at outlet of the impeller is converted into pressure energy before the water leaves the casing and enters the delivery pipe.

Suction pipe with a foot valve and a strainer:

A pipe whose one end is connected to the inlet of the pump and the other end dips into water in a sump is known as a suction pipe. A foot valve, which is non-return valve or one-way type of valve, is fitted at the lower end of suction pipe. The foot valve opens only in the upward direction. A strainer is also fitted at the lower end of suction pipe

Delivery pipe:

A pipe whose one end is connected to the outlet of the pump and the other delivers the water at the required height is known as delivery pipe.

1.2.2 Classification of Centrifugal Pump

Based on their utility, design and Constructional features, centrifugal pumps can be classified with respect to the following characteristics.

1.2.2.1 Working head

- **Low lift Centrifugal pumps**: Low lift centrifugal pumps are meant to work against heads up to 15m, Impeller is surrounded by a volute and there are no guide vanes.
- **Medium lift:** Medium lift centrifugal pumps are used to build up heads as high as 40m. They are generally provided with guide vanes.

- **High lift:** High lift centrifugal pumps are employed to deliver liquids at heads Above 40m, high pumps are generally multistage pumps because single impeller cannot build up such a high pressure

1.2.2.2 Number of stages

- **Single stage pump:** It has one impeller keyed to the shaft. This is generally horizontal but can be vertical also. It is usually low lift pump.

- **Multistage pump:** It has two or more impellers keyed to a single shaft enclosed in the same casing. Pressure is built up in steps. The impeller is surrounded by guide vanes and the water is led through a by-pass channel from the outlet of one stage to the entrance of the next until it is finally discharged into a wide chamber from where it is pushed on to the delivery pipe . These pumps are used essentially for high working heads and the number of stages depends on the head required.

1.2.2.3 Relative direction of flow through impeller

- **Radial flow pump:** It is that pump in which the liquid flows through the impeller in the radial direction only. Ordinarily all the centrifugal pumps manufacture with radial flow impeller.

- **Mixed flow pump: :** In mixed flow pumps the liquids flows through the impeller axially as well as radially i.e. there is a combination of radial and axial flows. A mixed flow pump is just a modification of radial flow type in this respect that the former is capable of discharging a large quantity of liquid.

- **Axial flow pumps:** In axial flow pumps the impeller is in the axial direction only. Axial flow pumps are usually designed to deliver very large quantities of liquid at relatively low heads

1.2.2.4 Number of entrance to impeller

- **Single entry or single suction pump:** In a single suction pump liquid is admitted from a suction pipe on one side of impeller.

- **Double suction pump:** In double suction pumps liquid enters from both sides of impeller. A double suction pump has an advantage that by this arrangement the axial thrust on the impeller is neutralized.

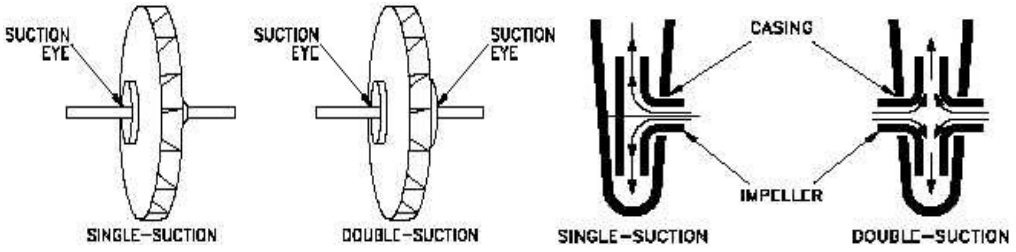

Figure 1.6 Single entry and double entry suction pump

1.2.2.5 Outlet blade angle

- **Backward Blade:** Outlet blade curves in a direction opposite to that of motion , & the angle between the blade tip & the tangent to rotor at exit is below 90 ($\beta_2<90$)
- **Radial Blade**: Liquid leaves the blade with relative velocity in a radial direction & angle $\beta_2=90$
- **Forward Blade:** Outlet tip of blade curves in the direction of motion & the angle between blade tip & the tangent to rotor at exit is obtuse ($\beta_2>90$).

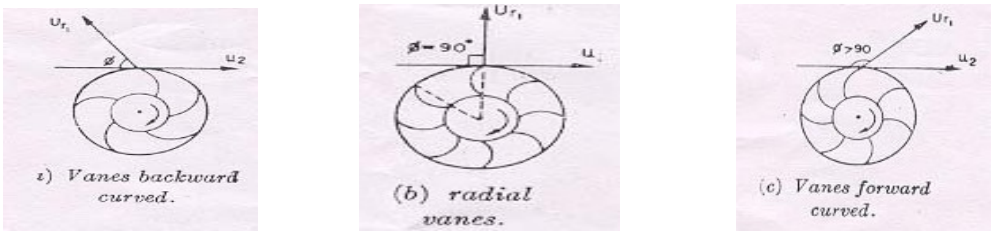

Figure1.7 Different type of outlet blade angle

1.2.2.6 Depending on the position of impeller

- Horizontal impeller shaft pump
- Vertical impeller shaft pump

The centrifugal pumps may be designed with either horizontal or vertical position of shaft, generally the pumps are provided with horizontal shaft. For deep wells and mines application the pumps with vertical shaft are more suitable.

1.2.2.7 Impeller

- **Shrouded or closed impeller:** It is an ordinary centrifugal pump is equipped with a closed impeller in which the vanes are covered with shrouds on both sides. This type is meant to handle non-viscous liquid such as ordinary water, hot water, hot oils and chemicals like acids etc,
- **Semi-Open Impeller:** The impeller which is shroud on one side only. This impeller is used for viscous liquid such as sewage; paper pulp etc, choice of material for manufacturer of impeller is influenced by chemical nature of liquid to be handled.
- **Open impeller.** The impeller is not provided with any shroud. Such pumps are used for handling mixture of water, sand, clay etc, it is generally made of forged steel.

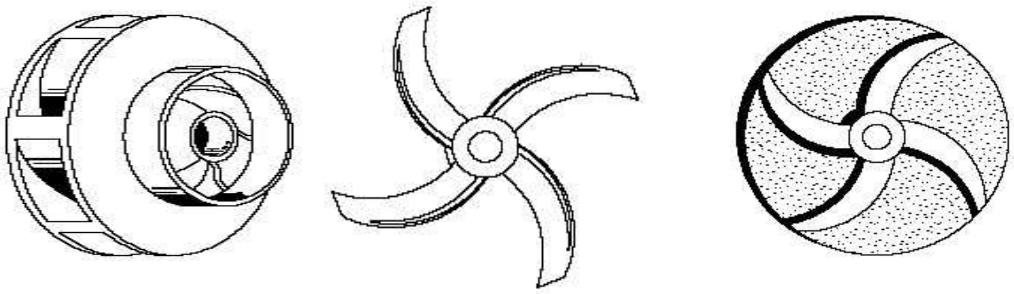

Figure 1.8 Different types of impeller

1.2.2.8 Casing

- **Volute casing**

  Volute casing is of spiral type in which area of flow increase gradually. The increase in the area of flow decreases the velocity of flow. The decrease in velocity increases the pressure of the water flowing through the casing. In case of volute casing the efficiency of the pump increase slightly as a large amount of energy is lost due to formation of eddies in this type of casing.

- **Vortex casing**

  If a circular chamber is introduced between the casing and the impeller, the casing is known as vortex casing. By introducing the circular chamber, the loss of energy due to formation of eddies is reduced considerably. Thus, the efficiency of the pump is more than the pump with volute casing.

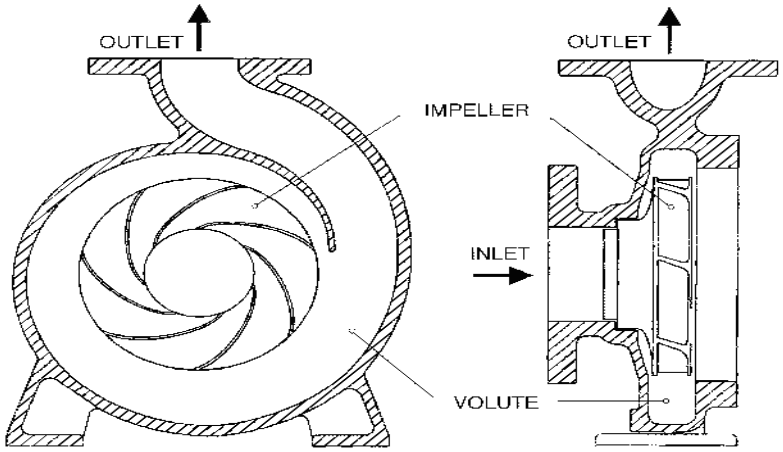

Figure 1.9 casing

- **Diffuser casing**

  In this type of casing, the impeller is surrounded by series of guide blades mounted on a ring, which is known as diffuser. The guide vanes are designed in such a way that water from the impeller enters the guide vanes without shock .Also the area of guide vanes increase, thus reducing the velocity of flow through guide vanes and consequently increasing the pressure of pressure of water. The water from the guide vanes then passes through the surrounding casing, which is concentric with the impeller.

1.2.3 Performance Characteristic of pump

A pump is usually designed for a particular speed, flow rate and head, but in actual practice the operation may be at some other condition of head, and for the changed condition the behavior of the pump is less efficient than the quantity the value of velocity of flow of liquid through impeller will be changed. As a result, the value of v, r and vr will be changed, and at the same time the loss will be increased so the efficiency of pump will lowered, therefore, in order to

predict the behavior and performance of a pump under varying condition, tests are performed, and the result of test are plotted, the curve thus obtained are known as characteristic curve of a pump. Characteristic curve are usually prepared for the centrifugal pumps are main and operating characteristic curve, constant efficiency curves, constant head & constant- discharge curve.

1.2.3.1 Main characteristics

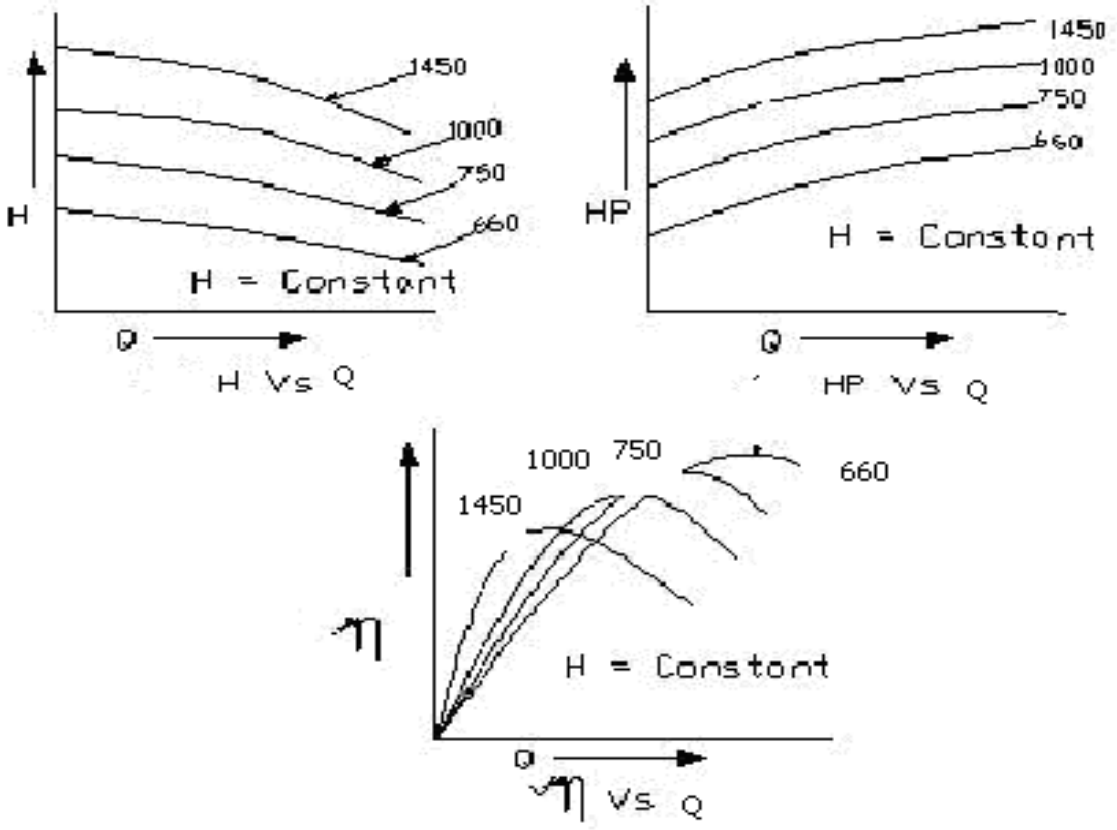

Figure 1.10 Main characteristic curves of centrifugal pump.

These are obtained by fixing the speed at some arbitrary value of and plotting separately H, HP, & η against Q. The rate of flow Q is varied by means of the quantity H, HP, η are calculated. A number of different values of N are chosen and one such set of curves is drawn for each speed.

1.2.3.1 Operating characteristics

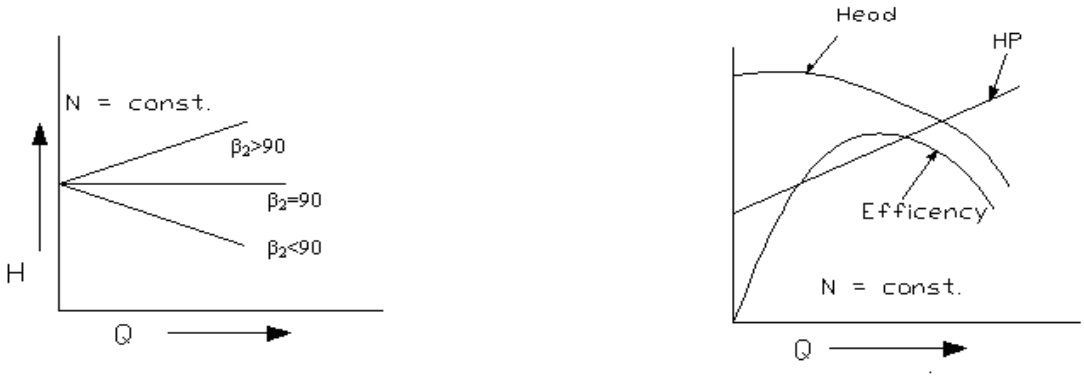

Figure 1.11 Operating characteristic curves of centrifugal pump

1.2.4 Centrifugal pump application

Pumps are used wherever any quantity of liquid must be moved from one place to another. Pumps are found in such services as steam power plants; water supply plants; sewage; drainage or irrigation; oil refineries, chemical plants and steel mills; food processing factories and mines; dredging or jetting operations; hydraulic power services and almost every ship whether driven by diesel or steam engine. While these pumps have much in common, they are varied to meet special requirements and particular needs of each service.

- Petroleum Industry
- Chemical Industry
- Textile Industries
- Paper Industry
- Sewage and Sump Services
- Irrigation, Drainage and Flood Control
- Mining and Construction

1.3 MOTIVATION OF THE PRESENT WORK

Computational fluid dynamics (CFD) analysis is being increasingly applied in the design and simulation flow in centrifugal pumps. Numerical simulation makes it possible to visualize the flow condition inside a centrifugal pump, and provides valuable information about the centrifugal pump's hydraulic design. By using simulation result to calculate or predict the performance of a centrifugal pump to replace or reduce the experiments in the process of pump design, a great deal of labor and facility will be saved, as well as its shortening design cycle. Therefore, great improvement on centrifugal pump design must be achieved by CFD analysis of inner flow inside a centrifugal pump and following application of its results in pump design processes.

The objective of the work is to model and numerically investigate the flow field inside the centrifugal slurry pump of pilot plant at IIT Roorkee using commercial CFD code FLUENT.

CHAPTER-2

LITERATURE REVIEW

S.Yedidiah[1][1996] u**sed** a novel approach for calculating the head developed by a centrifugal impeller. The approach was based on the fact that the head developed by an impeller depends on the shape of the total blade and not just upon the magnitude of its outlet angle.

Miner, S. M[2] [1997] has calculated numerically the flow field and pressure field within the rotor of an axial flow pump. Velocity and pressure profiles were developed on both sides of the impeller. It is observed that the value of tangential velocity increases from the centre line to the outer radius. The axial velocity profile shifts towards the outer radius because of the presence of nose on the hub. The use of coarse and fine mesh does not show significant difference in the values, thus even coarser mesh can be used.

Murugan, D. M. et al[3][1997] have observed flow using LDV system in the exit region of a radial inflow turbine at off-design operating condition. They investigated that the tangential velocities of the fluid exiting along the pressure surface were higher compared to those along the suction surface. The degree of swirl near the tip was high and radial velocities were low throughout the cross-section except pressure surface tip corner region which was caused due to the interaction of the tip clearance flow with the main flow.

Chung [4][1999] developed optimum design code of the pump. They determined the geometric and fluid dynamic variables under the appropriate design constraints. Optimization problem has formulated with a non-linear objective function to minimize losses, net positive suction head required and product price of a pump stage depending on the weighting factor selected as the design compromise. Optimal solution obtained, efficiency $NPSH_R$ depends design variable of centrifugal pump. Selected in the range of weighting factor 0 to 1.designer can easily find the optimum value of design variable to meet their particular requirement of pump design.

Majidi, K. et al[5] [2000] have observed the secondary flow in volute and circular casings of centrifugal pumps. The static pressure was not distributed uniformly at the outlet of the impeller which results in the radial thrust. The maximum relative velocity occurred at the periphery of the

impeller. The analysis shows that the curvature of the casings creates pressure gradients that cause vortices at cross-sectional planes of the casings.

Ogut, A. et al[6] [2000] have provided an insight into the effectiveness of fluid injection as a boundary layer control method in suppressing or eliminating flow separation in the vaned diffuser at off-design flow conditions. The reverse flow was observed along the hub and shroud walls. They also reduced the phenomenon of flow separation along the walls by injecting the fluid. The pressure recovery will be maximum if injection rate was 3% to the 60% of design flow rate.

J.J More[7][2001] The demand for higher efficiency and performance of modern centrifugal turbo machinery require a improve knowledge of critical design character in strength of material, aerodynamics and rotodynamics. While tremendous strides in a finite element stress analysis and CFD analysis have addressed the first two areas. The lack of accurate prediction tool for centrifugal impeller typically leaves rotodynamics out of the design loop. A commercial CFD code is adapted to solve the rotodynamic coefficient in a shrouded pump impeller. The code demonstrates close prediction of mean velocity profile in a complex flow filed of a grooved annular seal. Comparison to the experimental result of a boiler feet pump impeller show good overall correlation especially in a sub synchronous regime, which is important for good rotodynamic stability assessment.

Oh and Kim1[8] [2001] developed a design optimization code for mixed flow pump to determine the geometric and fluid dynamic variables under appropriate design constraints. Optimization problem has been formulated with a nonlinear objective function to minimize the fluid dynamics losses.

Wen Guang LI[9][2001] Had studied the flow of water as well as viscous oil in the 3 rectangular section of a volute of the centrifugal pump are measure by using two dimensional laser Doppler veloctimetry (LDV) in the best efficiency and part loading point respectively. The results show that the magnitude of tangential component of absolute velocity is one order larger than the rate of radial component. There are spiral motion in a section of volute. There is a secondary flow which is a pair of vortices with opposite rotating direction and in spiral motion in a section of volute. The flow of water or viscous oil in a volute is diffused at both best efficiency point and a

part loading point. The diffusion of the flow is weakened along the tangential direction of volute while pumping the high viscosity oil.

Jose et. al [10][2002] had shows the capability of a numerical simulation in capturing the dynamic and unsteady flow effect inside a centrifugal pump due to the impeller volute interaction. The object of the study is commercial centrifugal water pump with backward curved blades which is build with in a vane less single tongue volute. They concluded that the impeller volute interaction in a centrifugal pump is successfully predicted by a numerical model developed using a finite volume commercial code. Both experimental and numerical prediction shows the presence of spatial fluctuation pattern at the blade passing frequency as a function of flow rate. The unsteady calculation combined with the sliding mesh technique has proven to be a useful tool to investigate the flow field inside a centrifugal pump including the dynamic effect.

Akira. Goto et. Al[11] [2002] A computational aided design system has been developed for hydraulic parts of pump including impeller bowl diffuser volute and vened return channel. The key technologies include 3-D cad, model automatic grid generation, CFD analysis and 3-D inverse modeling. The design system is directly connected to rapid prototyping production system and flexible manufacturing system composed of a group of DNC machine and has been operated for actual daily design work. The key aspects of this new design system are efficient and systematic optimization of principal design parameters. However the strength of using the 3-D inverse design method is the fact that it is to apply establish design strategy such as a secondary flow control to other similar design and to construct more systematic and universal design

Gandhi et al.[12] [2002] have evaluated performance characteristics of a centrifugal slurry pump at different rotational speeds with water as well as solid-liquid mixture. They found that the affinity relations applicable to conventional pumps for head and capacity can be applied to slurry pumps handling water and slurries at low concentrations (<20% by weight). For higher solids concentrations, these relationships needed to be corrected by taking into account the effect of solids

Kato, C. et al.[13] [2003] have observed boundary interface between impeller and volute casing by using overset grids from dual frames of reference. The overall grid was composed of several grid

sets, and appropriate transactions take place at the interface regions. Large-eddy simulation was applied to the prediction of internal flows in a high–specific-speed, mixed-flow pump stage that possesses weak instability in its head-flow characteristics at low flow-rate ratios. The head-flow characteristics were also developed, although the large eddy simulation predicted the stall point at a lower flow-rate ratio than the measurements flow rate. The phase-averaged distributions of the meridional- and tangential-velocity components were also compared with those measured by an LDV.

Nursen, E. C. et al.[14] [2003] have developed an incompressible flow solver for the pump volute. The developed flow solver provides detailed pressure and velocity distribution information inside the volute, and the calculated results were verified by means of the experimental results.

Baun, D. O. et al[15] [2003] have observed the comparison between the characteristics of the lateral impeller forces and the hydraulic performances of four and five vane impeller operating in the spiral volute, concentric volute and double volute. The hydraulic performances of the two impeller designs were compared in each of the three different volute configurations. The force characteristic for the four vane impeller was similar to the five vane impeller in each respective volute casing. The best efficiency point shifts to a lower flow rate and the relatively rapid droop in the head and efficiency characteristics of the double volute at high flows was likely to be the result of increased volute losses. The losses in the double volute will increase over the single volute because of more wetted surface and two tongues, which result in twice the incidence losses as compared to the single volute.

Zhou, W. et al[16] [2003] have used a CFD code to study three-dimensional turbulent flow through water-pump impellers during design and off-design conditions. Three different types of centrifugal pumps were considered in this simulation. One pump had four straight blades and the other two had six twisted blades. It was found that pumps having six twisted blades were better than those for pumps with straight blades, which suggests that the efficiency of pumps with twisted blades will also be higher than that of pumps with straight blades. It was also found that when the flow rate decreased below a certain value of the design flow rate, backflow occurred near the pressure surface of the pump impeller.

Kato, C. et al[17] [2003] have observed boundary interface between impeller and volute casing by using overset grids from dual frames of reference. The overall grid was composed of several grid sets, and appropriate transactions take place at the interface regions. Large-eddy simulation was applied to the prediction of internal flows in a high– specific-speed, mixed-flow pump stage that possesses weak instability in its head-flow characteristics at low flow-rate ratios. The head-flow characteristics were also developed, although the LES predicted the stall point at a somewhat lower flow-rate ratio than did the measurements. The phase-averaged distributions of the eridional- and tangential velocity components were also compared with those measured by an LDV.

Nursen, E. C. et al[18] [2003] have developed an incompressible flow solver for the pump volute. The flow inside the volute of a centrifugal pump was three dimensional and, depending upon the position of the inlet relative to the cross-section center line, a single or double swirling flow occurs. The developed flow solver provides detailed pressure and velocity distribution information inside the volute, and the calculated results were verified by means of the experimental results. Calculations were performed at three different mass flows, one of which corresponds to the design's point mass flow. The calculated volute flow conditions namely, the variation in static pressure and total pressure and the through flow and swirling component of the flow velocity over the cross-sections, which were located at various circumferential positions.

Kadambi et al.[19] [2004]) have used Particle Image Velocitimetry to investigate the velocities of the slurry in the impeller of a centrifugal slurry pump for sodium-iodide solution (NaI) and 500micron glass beads slurry. The experiments conducted at 725 rpm, 1000rpm speed, and1%, 2%, 3% volumetric concentration. They observed that the in clear fluid flow conditions for both the pump rpm, flow separation takes place on the suction side of the blade in the region below the blade tip. For the same flow conditions, the flow moves smoothly along the suction side of the blade depicting a recirculation zone. The intensity of this recirculation zone decreases at the higher concentration of 3% due to particle inertia effects. On the pressure side of the blade the particles are pushed along the blade surface and can result in the frictional wear.

Hergt, P. et al.[20] [2004] have observed the unsteady velocity, pressure and flow angle at the impeller outlet of a centrifugal pump with and without volute casing at five operating points using the hotwire technology and a fast response single hole cylindrical probe. The test fluid was

air. While the velocities and pressures depend only on the axial coordinate and were rotationally symmetrical. If there was no casing around the impeller, the influence of the volute on the circumferential distribution of these quantities increases with the deviation of the operating point from the design point.

J. H. Horlock el. Al [21] [2005] after the development of gas turbine, many empirical design were used for example in obtaining the fluid deflection using the deviation from the blade angle in the assumption of zero radial velocity and in expression for clearance loss. The validity of some of this rules and the basic fluid mechanics behind them is examined by use of modern idea and CFD code and concluded that the interaction of leakage flow, cooling flow and cavity flow with the main gas path flow has usually been neglected in past but its importance is starting to be realize. Such flow can interact with the main stream flow to produce shear layers which contains vorticity and hence generate additional secondary flow and losses.

Robert Rey et al [22] [2005] studied a 3D-CFD simulation of the impeller and volute of a centrifugal pump has been performed using CFX Codes. The pump has a specific speed of 32 (metric units) and an outside impeller diameter of 400 mm. First, a 3D flow simulation for the impeller with a structured grid is presented. A sensitivity analysis regarding quality and turbulence models were also performed. The final impeller model obtained was used for a 3D Quasi-unsteady flow simulation of the impeller volute stage. A procedure for designing the volute, The nonstructural grid generation in the volute, and the interface flow passage between the impeller and volute are discussed. This flow simulation was carried out for several impeller blades and volute tongue relative positions. As a results, Velocity and pressure field were calculated for different flow rates, Akkowing to obtain the radial trust on the pump shaft.

Asuaje et al. [23] [2005] carried out study on 3D-CFD simulation of the impeller and volute casing of a conventional centrifugal pump by using CFX code. A three-dimensional computational fluid dynamics simulation was carried out on an impeller of known geometry from which values of slip factor were calculated for both single and two phase flow. This flow simulation was carried out for several impeller blades and volute tongue relative positions. They obtained slip factor as a function of the specific capacity and the gas void fraction. Velocity and pressure field were calculated for different flow rates, allowing obtaining the radial thrust on the pump shaft.

Min-Guan [24][2007] have observed the phenomena of two-phase flow with salt crystallizing in the chemical pump. The 3-D turbulent flow in the impeller of chemical pump was simulated at the condition of rinsing. The internal flow between the impellers of chemical pump was investigated. Based on the Reynolds-Averaging Navier-Stokes (RANS) equations and the standard k-ε two equations turbulent model, the simulations of turbulent flow between the impellers were performed using Fluent under different operating conditions. Based on the analysis of the calculated velocity and pressure profiles in the chemical pump and experimentally observed phenomenon of flow impact, secondary flow, and recirculation, some design improvements were proposed.

Cheah et al.[25] [2007] has performed study on the numerical simulation of centrifugal pump performance by using commercial code CFX. Computation is carried out with a multiple rotating reference frame (MRF model) approach because the impeller flow field is in a rotating frame whereas the intake section and volute casing are in stationary frame. The meshes of three computational domains, the intake section, impeller, and volute casing and intermediate plates are generated separately. Unstructured mesh with tetrahedral element is used in all three computational domains of centrifugal slurry pump

A.Roudnev [26] [2007] The casing wear modeling can be carried out by using commercial CFD codes. have analyzed numerical method for predicting casing wear in a centrifugal slurry pump is based on a sliding erosion model. They are used CFD multiphase simulation using the Eulerian-Eulerian approach. It is used successfully to determine the velocity fields and solid concentration in the centrifugal pump, allowing for accurate predictions of casing wear patterns resulting from sliding abrasive wear

J. Amaral- Teixeira[27] [2007] have study a numerical investigation of the time variation of pressure within the complete centrifugal pump was undertaken. A range of parameters and three flow rates were investigated and the pulsations were extracted at 15 different locations covering important pump regions. The transient flow results compared reasonably with experimental data obtained in a limited experimental survey and clearly indicated the pump locations experiencing the largest pulsating levels. It was also noted that monitoring pulsating at the top dead centre of the pump volute casing would provided a better indication of internal pump pulsating than monitoring at the discharge.

Feng, J. et al[28] [2007] have investigated the unsteady flow and the pressure fluctuation in radial diffuser pumps. Calculations were performed at different operating points, radial gaps, and blade number between the impeller and diffuser. Computational results show that a jet-wake flow structure was observed at the impeller outlet. The biggest pressurefluctuation on the blade was found to occur at the impeller trailing edge, on the pressure side near the impeller trailing edge, and at the diffuser vane leading edge. All the flow rates, blade number configuration, and radial gaps influence significantly the pressure fluctuation and associated unsteady effects in the diffuser pumps

Hofmann, M. et al[29] [2007] have done both experimental and numerical work on 3D cavitating flows. To observe experimental results a high speed video with the light sheet illumination were used. Numerical calculation was based on the 3D code, to predict the cavitations behavior in turbo-machinery. This model was applied to the centrifugal pump geometry. Non-cavitating and cavitating conditions were investigated. Calculations were found to be in good agreement with experimental measurements and visualizations. Three regions for the occurrence of cavitation were observed, first at the shroud blade interface, second at the suction side of blade, and third were at the hub at the inlet of the blade

Younsi, M. et al[30] [2007] have observed the splitter blades effect on the performance of a centrifugal pump through both numerical simulation and experimental results. The analysis shows that, by adding splitter blades to the impeller, the impeller periphery velocities and pressures become more homogeneous. The influence of splitter blades on the velocity and pressure fields in a centrifugal impeller has been analyzed by means of 3D simulations. The splitter blades increases the head rise compared to the original impeller because of the impeller slip factor which helps conduction of the flow. But the efficiency was not improved since the hydrodynamic losses were greater. It decreases the pressure fluctuations and reorganizes more conveniently the flow at the volute outlet. But for all the studied flow rates it increases the interaction between the volute tongue and the flow. The consequence was an increase of the radial thrust.

John S. Anagnostopoulos[31][2009] A numerical methodology is developed to simulate the turbulent flow in a 2-Dimensional centrifugal pump impeller and to compute the characterstics performance curve of the entire pump. The flow domain is discretized with a polar, Cartesian

mesh and the Reynolds-averaged Navier-Strokes (RANS) equations are solved with the control volume approach and the K-E turbulence model. Advanced numerical techniques for adaptive grid refinement and for the treatment of grid cells that do not fir the irregular boundaries are implemented in order to achieve a fully automated grid construction for an impeller design, as well as to produce results of adequate precision and accuracy. After estimating the additional hydraulic losses in the casing and the inlet and outlet sections of the pump, the performance of the pump can be predicted using numerical results from impeller section only. The graduations of various energy losses coefficients involved in the model is carried out for a commercial pump, for which there are available measurements. The predicted overall efficiency curve of the pump was found to agree very well with the corresponding experimental data. Finally, a numerical optimization algorithm based on the unconstrained gradient approach is developed and combined with the evolution software in order to find the impeller geometry that maximizes the pump efficiency, using as free design variables the blade angles at the leading and the trailing edge. The result verified that the optimization process can converge very fast and to reasonable optimal values.

M. Pathak et al [32] (2009) a computational investigation of two phase (solid -liquid) slurry flow around a square shaped obstruction in the bottoms wall of a rectangular duct is made. The slurry flow having low particle concentration consists of zinc tailing and water where water is consider as primary phase and zinc tailing as a secondary phase the algebraic slip mixture model is used to solve the two phase governing equation and standard k-e model is used to resolve the turbulence of the flow field and concluded that the complex interaction occurs between the two phase occurred in the downstream of the obstruction. The slip velocity is very small and effect of this velocity is very small in homogeneous and heterogeneous flow.

Kalekudithi ekambara et al [33](2009) the .behavior of horizontal solid_ liquids(slurry) pipeline flow was predicted using a transient three dimension hydrodynamic model based on the kinetic theory of granular flow. computational fluid dynamics simulation result obtained using a commercial CFD software package .the simulation were carried out to investigate the effect of in solid volume concentration (8 to 45%),practical size (90 to 500um) mixture velocity (1.5 to 5.5m/s) and pipe diameter 50 to 500mm..and concluded that the CFD model describe here is

capable of predicting particle concentration profile for fine particle slurry .it also concluded that when particle are coarse and concentrated profile are primary depends upon the in situ solid volume fraction

Ekambara et al[34] [2009] carried out study of hydrodynamic simulation of horizontal slurry pipeline flow using ANSYS-CFX. Numerical simulation of slurry flow through pipeline provides information of solid-liquid mixture behavior that assists simulation of centrifugal pump handling slurry. The behavior of horizontal solid-liquid (slurry) pipeline flows is predicted using a transient three-dimensional (3D) hydrodynamic model based on the kinetic theory of granular flows. The simulated results indicate that the particles are asymmetrically distributed in the vertical plane with the degree of asymmetry increasing with increasing particle size. Once the particles are sufficiently large, concentration profiles are dependent only on the solid volume fraction. The numerical computation is carried out with a multiple rotating reference frames because the impeller flow field is a rotating frame whereas the intake section and volute casing are in stationary frame. For solid – liquid mixture handling, mixed multiphase model or Eulerian model is used.

Behrouz et al.[35] [2010] have carried out study on three-dimensional simulation of turbulent fluid flow to predict velocity and pressure fields for a centrifugal pump. A commercial CFD code was used to solve the governing equations of the flow field. They applied three known turbulence models standard k − ε, RNG and RSM, and found that standard k- ε gives better results. The effect of numbers of blades on the efficiency of pump was carried out. The number of blades was changed from 5 to 7 and they observed the impeller with 7 blades has the highest head coefficient.

CHAPTER-3
COMPUTATIONAL FLUID DYNAMICS

3.1 INTRODUCTION

Computational fluid dynamics (CFD) is one of the branch of Engineering, Finding numerical solutions of governing equations, using high-speed digital computer.CFD uses numerical methods to solve the fundamental nonlinear differential equations that describe fluid flow, for predefined geometries and boundary conditions. The result is a wealth of predictions for flow velocity, temperature, density, and chemical concentrations for any region where flow occurs. A key advantage of CFD is that it is a virtual modeling technique with powerful visualization capabilities and engineers can evaluate the performance of a wide range of system configurations on the computer without the time,

Computational Fluid Dynamics (CFD) provides a qualitative or quantitative prediction of fluid flows by means of:

- Mathematical modeling (partial differential equations)
- Numerical methods (discretization and solution techniques)
- Software tools (solvers, pre- and post processing utilities)

Fluid flows and related phenomena can be described by partial differential (or integro differential) equations, which cannot be solved analytically except in few special cases. To obtain an approximate solution numerically, we have to use a discretization method which approximates the differential equations by a system of algebraic equations, which can then be solved on a computer. The approximations are applied to small domains in space and/or time so the numerical solution provides results at discrete locations in space and time. Much as the accuracy of experimental data depends on the quality of the tools used, the accuracy of numerical solutions is dependent on the quality of discretization used.CFD is finding its way into process, chemical, civil, and environmental engineering. Optimization in these areas can produce large savings in equipment and energy costs and in reduction of environmental pollution.

3.2 CFD METHODLOGY

In order to obtain better design in CFD, following methodology is used for designing of any components.

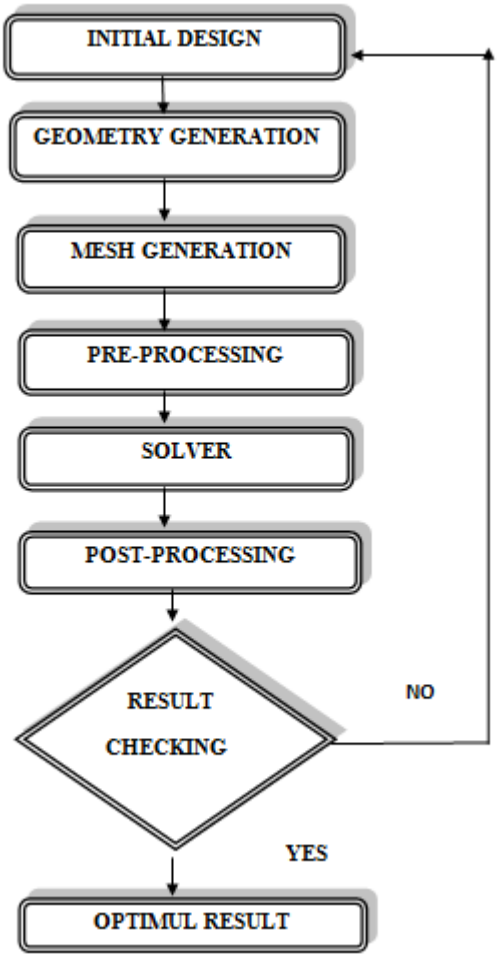

Figure 3.1 Flow chart of CFD

3.2.1Initial design

In order to obtain better design in CFD, following procedure is applied so that fluid flow can easily be modeled. Initial design of the model is a planning decision and the Geometry is generated depending on these initial design considerations, using either CFD Modeling tools or

other Design, which is used to input the problem geometry, generates the grid; define the flow parameter and the boundary conditions to the code.

3.2.2 Geometry generation.

The geometry of design needs to be created from the initial design. Any modeling software can be used for modeling and then shifted to other simulation software for analysis purposes.

3.2.3 Mesh generation

Mesh generation (Girding) is the process of subdividing a region to be modeled into a set of small control volumes. Associated with each control volume there will be one or more values of the dependent flow variables (e.g., velocity, pressure, temperature, etc.) Usually These represent some type of locally averaged values. Numerical algorithms representing approximations to the conservation laws of mass, momentum and energy are then used to compute these variables in each control volume. Meshing is a method to define and break up the model into small elements.

3.2.4 Pre-processor

Which is used to input the problem geometry, generates the grid; define the flow parameter and the boundary conditions to the code.

3.2.5 Flow solver

Which is used to solve the governing equations of the flow subject to the Conditions provided there are three different methods used as a flow solver:

- **Finite difference method**: Finite difference method utilizes the Taylor series expansion to write the derivatives of a variable as the differences between values of the variable at various points in space or time.
- **Finite element method**: In the finite element method, the fluid domain under Consideration is divided into finite number of sub-domains, known as elements. A Simple function is assumed for the variation of each variable inside each element. The Summation of variation of the variable in each element is used to describe the whole Flow field.
- **Finite volume method**: The finite volume method is currently the most popular Method in CFD. The main reason is that it can resolve some of the difficulties that the other two methods have. Generally, the finite volume method is a special case of Finite element.

3.2.6 Post-processor

Post processor is used to massage the data and show the results in graphical and easy to read format

3.3 GOVERNING EQUATIONS IN CFD

The physical aspects of any fluid flow are governed by the following three fundamental Principles:

a) Conservation of mass

b) Conservation of momentum (Newton's second law)

c) Conservation of energy (First law of thermodynamics)

3.3.1 The mass conservation equation

The law of mass conservation is a general statement of kinematic nature, i.e. independent of the nature of the fluid or of the forces acting on it. It expresses the empirical fact that in a fluid system, mass cannot disappear from the system, nor be created. The quantity U is, in this case, the specific mass, $U = \rho$ in kg/m3.As noted , no diffusive flux exists for the mass transport, which means that mass can only be transported through convection. With the convective flux defined by $FC = \rho v$ and in absence of external mass sources, the general integral mass conservation equation then becomes in differential form

This equation is also called the continuity equation

$$\frac{\partial \rho}{\partial t} + \nabla . (\rho \vec{v}) = S_m \tag{3.1}$$

The source S_m is the mass added to the continuous phase from the dispersed second phase (e.g. due to vaporization of liquid droplets) and any user-defined sources. For Steady state compressible fluid flow the continuity equation is given by;

$$\rho(\nabla . \vec{v}) = 0 \tag{3.2}$$

Where,

$$\nabla = \frac{\partial}{\partial x_i}\hat{\imath} + \frac{\partial}{\partial x_j}\hat{\jmath} + \frac{\partial}{\partial x_k}\hat{k}$$

And

$$\vec{v} = u_i\hat{\imath} + u_j\hat{\jmath} + u_k\hat{k}$$

3.3.2 Conservation of momentum

Conservation of momentum in an inertial (non-accelerating) reference frame is described as

$$\frac{\partial}{\partial t}(\rho.\vec{v}) + \nabla.(\rho\vec{v}\vec{v}) = -\nabla p + \nabla.(\bar{\bar{\tau}}) + \rho\vec{g} + \vec{F} \quad (3.3)$$

Where

$\rho\vec{g}$ =Gravitational body force

F=external body forces (e.g. that arise from interaction with the dispersed phase), respectively. F also contains other model-dependent source terms such as porous media and user-defined sources.

The stress tensor $\bar{\bar{\tau}}$ is given by

$$\bar{\bar{\tau}} = \mu\left[(\nabla\vec{v} + \nabla\vec{v}^{t}) - \frac{2}{3}\nabla.\vec{v}I\right] \quad (3.4)$$

Where, the second term on the right hand side is taken for considering the effect of volume dilation.

For steady state incompressible fluid flow, the momentum conservation equation is given by

$$\nabla.(\rho\vec{v}\vec{v}) = -\nabla p + \nabla.(\bar{\bar{\tau}}) + \rho\vec{g} + \vec{F} \quad (3.5)$$

3.3.3 Conservation of energy

First law of thermodynamics applied to closed process, i.e. system taken through a complete cycle

$$\int (dQ - dW) = 0 \quad (3.6)$$

Change in internal energy during change in state from one point to another in the cycle

$$dE = dQ - dW \quad (3.7)$$

For a steady flow process the conservation of energy per unit time is regarded, i.e. conservation of power.

$$dE = \dot{m} . (dh_0 + g.dZ) = \dot{Q} - \dot{W} \quad (3.8)$$

Where,

dh_0 = the change in total enthalpy

g.dZ = change in specific potential energy.

Apart from hydraulic machines the latter can be neglected. Furthermore the process can be assumed as adiabatic leading to the conservation of energy for a steady turbo machine being written as

$$\dot{W} = \dot{m}. (h_{01} - h_{02}) \quad (3.9)$$

For work absorbing machines (compressors, pumps) $h_{01} < h_{02} \Rightarrow W < 0$ (3.10)

3.5 TYPES OF BOUNDRY CONDITION

The following boundary conditions at the walls are used with the equations of motion

- No slip conditions

  At fluid wall interface, there must be no slip

$$\vec{V}_{fluid} = \vec{V}_{wall}$$

- Inlet condition
- Outlet condition,
- Pressure and velocity
- Rotation about the axis direction
- Amount of mass flow at inlet and out let

3.6 TURBULENT MODELING

Turbulent Fluid flow is an irregular condition of flow in which the various quantities show a random variation with time and space coordinates, so that statistically distinct average values can be obsevered .A Fluid motion in which velocity, pressure, and other flow quantities fluctuate irregularly in time and space.

Example :of turbulent flow.

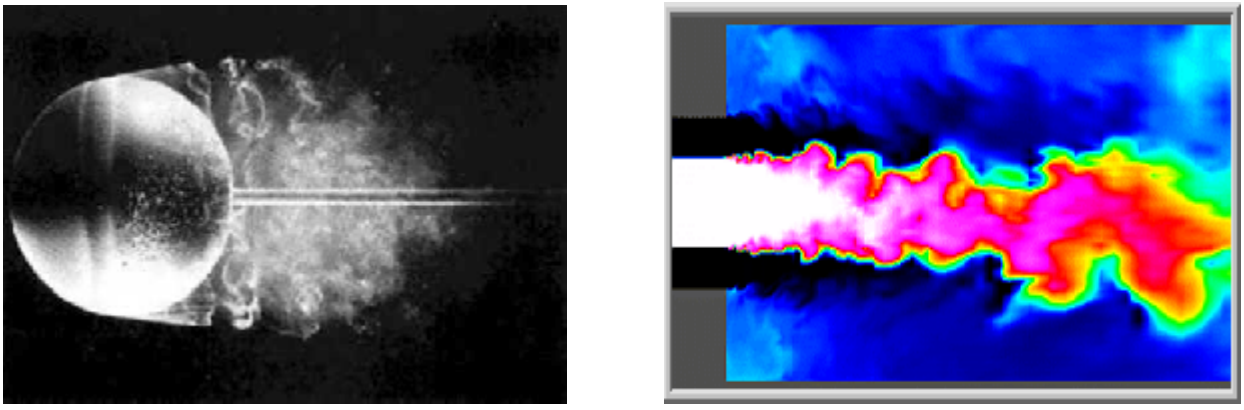

Figure 3.2 Turbulent Flow

Turbulent model:

Turbulence consists of fluctuations in the flow field in time and space. It is a complex Process, mainly because it is three dimensional, unsteady and consists of many scales. It can have a significant effect on the characteristics of the flow. Turbulence occurs when the inertia forces in the fluid become significant compared to viscous forces, and is characterized by a high Reynolds Number In turbulent flow we usually divide the variables in two components, one time-averaged part $\vec{U}$, which is independent of time (when the mean flow is steady), and other the fluctuating part u.

$$U = \vec{U} + u \tag{4.1}$$

The reason for decomposing the variables in two parts is:

- While measuring the flow quantities we are usually interested in the mean values rather that the time histories
- To solve the Navier-Stokes equation numerically it would require a very fine grid to resolve all turbulent scales and it would also require a fine resolution in time (turbulent flow is always unsteady).

3.6.1Types of turbulent modeling

There are many types of turbulent model in turbulent modeling. The four models are given below.

- **Zero-Equation Models**
- **One-Equation Models**
- **Two Equation Models**
- **Reynolds Stress Model**

3.6.1.1 Zero-Equation Models

The zero-equation model is equation wherein the turbulent fluctuating co-relation is related to the mean flow field quantities by algebraic relation. The underlying assumption in zero equation models is that the local rate of dissipation of turbulent are approximately equal and they do not include the convection of turbulent. And these models are mathematically simple. Generally most of the models employ an inner region/outer region formulation to represents mixing length. A commonly used model utilizes an exponential function for the inner region, where as the outer region is proportional to the boundary layer thickness.

Advantages ;

$$\varepsilon_i = l.l\left(\frac{\partial \bar{u}}{\partial y}\right)$$

- Simplest of Models satisfying the requirements.

Disadvantages;

- Some ad hoc assumptions have to be made regarding boundary layer and velocity.

3.6.1.2 One-Equation Models:

In these models a transport equation is solved for a turbulent quantity (usually the turbulent kinetic energy) and a second turbulent quantity (usually a turbulent length scale) is obtained from an algebraic expression. The turbulent viscosity is calculated from Boussinesq assumption.

Spalart-Allmaras model

Spalart-Allmaras model is a one equation model which solves a transport equation for a viscosity-like variable $\tilde{\nu}$. This may be referred to as the Spalart-Allmaras variable the turbulent eddy viscosity is given by.

$$\nu_t = \tilde{\nu} f_{v1}, \quad f_{v1} = \frac{\chi^3}{\chi^3 + C_{v1}^3}, \quad \chi := \frac{\tilde{\nu}}{\nu} \tag{4.3}$$

Advantages;

- Additional assumptions can be avoided.
- Break from the equilibrium concepts in a practical consideration.

Disadvantages;

- The length scale is still an algebraic quantity.
- Computationally more difficult

3.6.1.3 Two Equation Models:

These models fall into the class of eddy viscosity models. Two transport equations are derived which describe transport of two scalars, for example the turbulent kinetic energy K and its dissipation ε. The Reynolds stress tensor is then computed using an assumption which relates the Reynolds stress tensor to the velocity gradients and an eddy viscosity. The latter is obtained from the two transported scalars. Two equation models are further divided into two main models.

- **K-epsilon model.**
- **K-omega model**

K-epsilon model:

This is two-transport-equation model solving for kinetic energy k and turbulent dissipation ε. turbulent dissipation is the rate at which velocity fluctuations dissipate. This is the default k–ε model. And one of the most prominent turbulence models, the *k* -e (*k*-epsilon) model, has been Implemented in most general purpose CFD codes and is considered the industry standard model. It has proven to be stable and numerically robust and has a well established regime of predictive capability. For general purpose simulations, the model offers a good compromise in terms of accuracy and robustness.

The k- Epsilon model introduces two new variables into the system of equations.

And the momentum equation became

$$\frac{\partial \rho U}{\partial t} + \nabla \bullet (\rho U \otimes U) - \nabla \bullet (\mu_{eff} \nabla U) = -\nabla p^{'} + \nabla \bullet (\mu_{eff} \nabla U)^{T} + B \qquad (4.4)$$

Where

B is the sum of body forces,

μ_{eff} is the effective viscosity accounting for turbulence,

p' the modified pressure

Advantages:

- Relatively simple to implement.
- Leads to stable calculations that converge relatively easily.
- Reasonable predictions for many flows.

Disadvantages:

- Poor predictions for.
    - Swirling and rotating flows.
    - Flows with strong separation.
    - Axis symmetric jets.
    - Certain unconfined flows.
    - Fully developed flows in non-circular ducts.
- Valid only for fully turbulent flows.
- Simplistic ε equation.

K-omega model

This is two-transport-equation model solving for kinetic energy k and turbulent frequency ω. This is the default k–ω model. This model allows for a more accurate near wall treatment with an automatic switch from a wall function to a low-Reynolds number formulation based on grid spacing .one of the advantages of the formulation k–ω is the near wall treatment for low-Reynolds number computations. The model does not involve the complex non-linear damping functions required for the k–ω model and is therefore more accurate and more robust The models assumes that the turbulence viscosity is linked to the turbulence.

Kinetic energy and turbulent frequency via the relation:

$$\mu_t = \frac{k}{w} \tag{4.5}$$

μ = turbulence viscosity

K is the turbulence kinetic energy and is defined as the variance of the fluctuations in velocity

w=turbulence frequency.

Advantage

- It is modified version of k-epsilon.
- Leads to stable calculations that converge relatively easily.

Disadvantage

- It has to solve two (PDE).
- Valid only for highly turbulent flow

3.6.1.4 Reynolds stress model

Reynolds stress model closes the Reynolds-Averaged Navier-Stokes equations by solving additional transport equations for the six independent Reynolds stresses. Transport equations derived by Reynolds averaging the product of the momentum equations with a fluctuating property. The exact equation for the transport of the Reynolds stress R_{ij} :

$$\frac{DR_{ij}}{Dt} = P_{ij} + D_{ij} - \varepsilon_{ij} + \Pi_{ij} + \Omega_{ij}$$

This equation can be read as:

Rate of change of $R_{ij} = \overline{u_i' u_j'}$ plus

Transport of R_{ij} by convection, equals

Rate of production P_{ij}, plus

Transport by diffusion D_{ij}, minus

Rate of dissipation ε_{ij}, plus

Transport due to turbulent pressure-strain interactions π_{ij}, plus

Transport due to rotation Ω_{ij}.

Advantages

- More General than Eddy-Viscosity Models.

- Better Prediction for flow with sudden changes.
- Possible Ultimate turbulence models.

Disadvantages

- None of the equations can be solved exactly.
- Computational difficulty because of more no. of PDE

3.6 APPLICATION OF CFD

CFD is one of the most applicable techniques that are being used excessively in engineering application. Some of the application of CFD is given below.

Aerospace application;

CFD is now widely used in aerospace application for the purpose of predicting components performance and as an integral part of the design cycle. An example of flow around a complete aerospace is given in figure 3.3

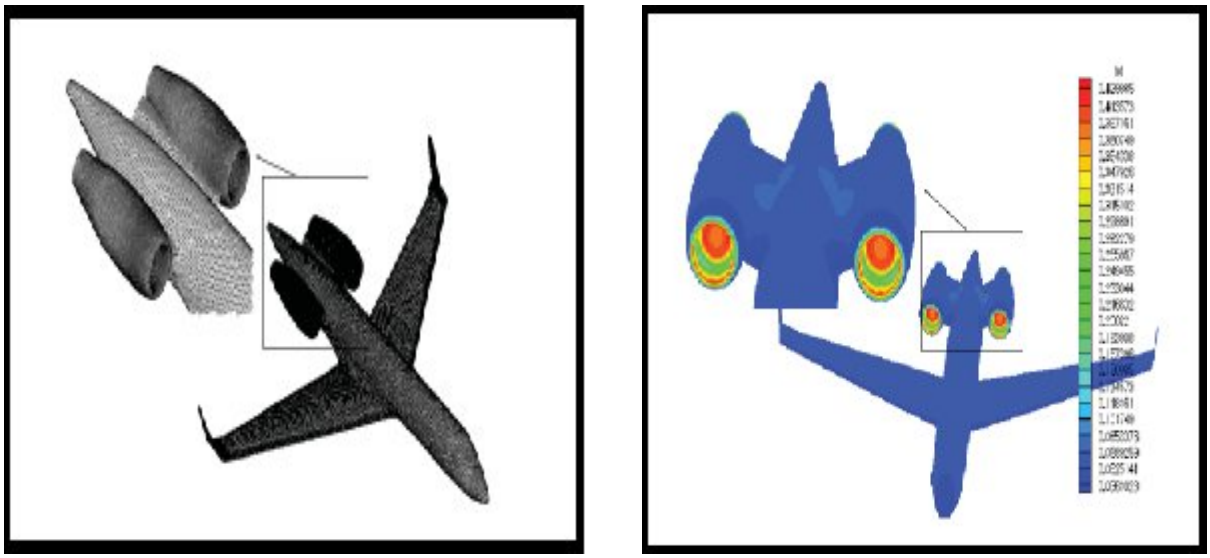

Figure3.3 Grid and flow simulation of aircraft

Automobile application;

In automotive, CFD is being used for many applications including engine components auxiliary system and also for modeling of aerodynamics of car to minimize drag and optimize the down force under different operating condition.

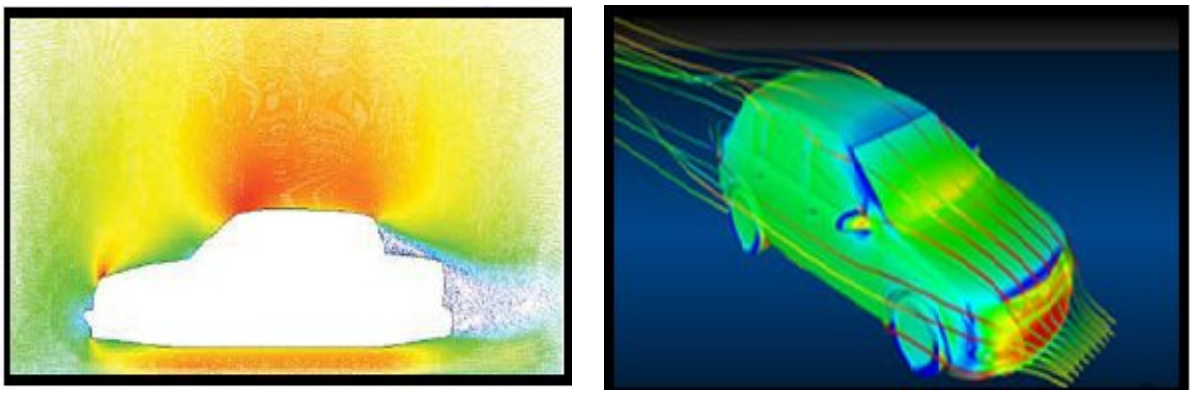

Figure 3.4 Path line and flow around a car

Biomedical application;

In biomedical application, CFD is now being used to model the flow in heart and vessels the flow of blood in heart assist device and various other fluid flow equipment such as drug and inhaler.

Turbo machine application;

In designing of turbo machinery CFD is used for finding the fluid flow inside turbo machine such as, pump, blowers, centrifugal fan.

CHAPTER 4

MODELING OF PUMP COMPONENTS

4.1 MODELING OF THE PUMP COMPONENTS

To study the numerical analysis on the pump, the dimension data of the pump was required to generate a model in the software. For taking the dimensions of components reverse engineering techniques were used. The pump was first disconnected from the pipes of the test loop and the water in the pump assembly was drained. The pump assembly was disassembled and all the parts were separated. The assembly consist the casing, impeller and suction. Since the pump was firmly placed on the foundation the suction passage extending from the flange to the frame was not removed.

4.2 DIMENSIONING

After the pump was disassembled, the task of taking dimensions of each component was divided in two phases.

1. The dimensions that could be taken directly like impeller outer diameter, casing outlet diameter, etc were taken using vernier calipers and steel rule.
2. For dimensions that could not be taken directly with instruments moulds of plaster of Paris and clay were made.

Impeller:

The impeller of pump is the enclosed type and has 5 vanes. The impeller tail extends from the center of the head through the discs till the suction passage where it rests on a disc connected to the shaft and embedded in the inlet passage. The tail section is circular in shape; this section has a constant diameter over a certain length and increases gradually over the end forming a bell

mouth at the end. This bell mouth lies in the suction passage from where the flow enters the pump. The main purpose of the giving bell shape to the tail of the impeller is the smoothening of the flow to ensure uniform feed to the impeller. A fillet is given at the inlet in the impeller head where the flow enters the vanes. Due to this fillet the width of the vane increases at the inlet. Since the impeller is closed type and the vane at inlet is wider than the outlet, it was not possible to measure the dimensions at the impeller inlet. The profile of the vane at inlet was reconstructed by making a mould out of m-seal. The other parts of the impeller were modeled using plaster of paris moulds. The dimensions were then taken from these moulds by plotting them on the graph. Points were marked on the graph sheet with respect to a reference. These points were then plotted in the software following which a curve with a suitable radius was fitted through the points to get the smooth surface.

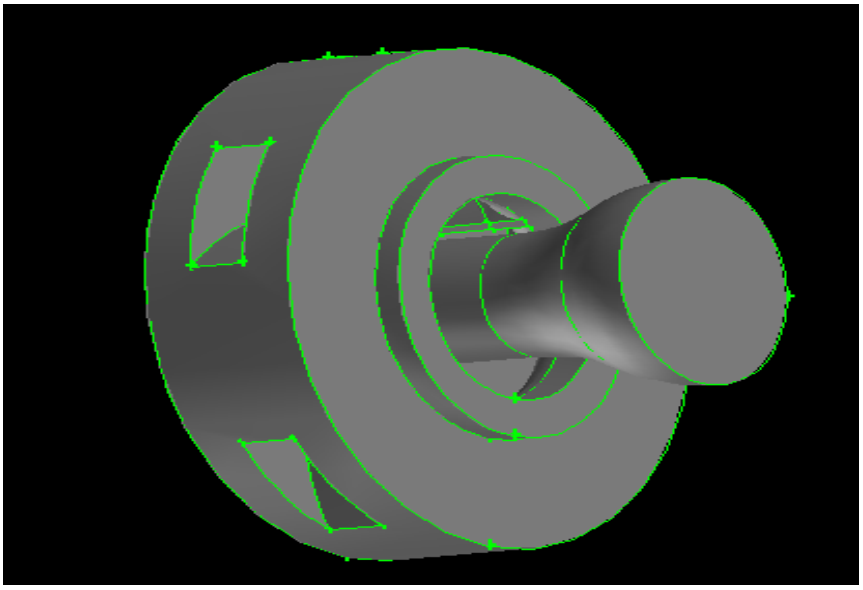

Figure 4.1 Cad model of Impeller

Casing

The casing is of semi-volute type having 275 mm base circle diameter and 11 degrees tongue angle. The casing was also modeled by making plaster of Paris moulds. For the purpose, the casing was divided into 12 sectors each spanning over 30 degrees. Once divided moulds of each

of these sectors were casted. The moulds were not casted for the entire sector but only for the area beyond the base circle, this was done to optimize the requirement of plaster of paris and also because only the area which is increasing was required. These 12 sectors were then put together to reconstruct the casing and check the conformation with the casing. These sectors were then grinded on the edges to get a clear cross-section on the graph. Each sector was then drawn over a base circle in the software. The cross-section was drawn by connecting the points with Nerbs. Once the cross-section of each sector was made, the casing was constructed with the bottom up approach by creating faces and volumes.

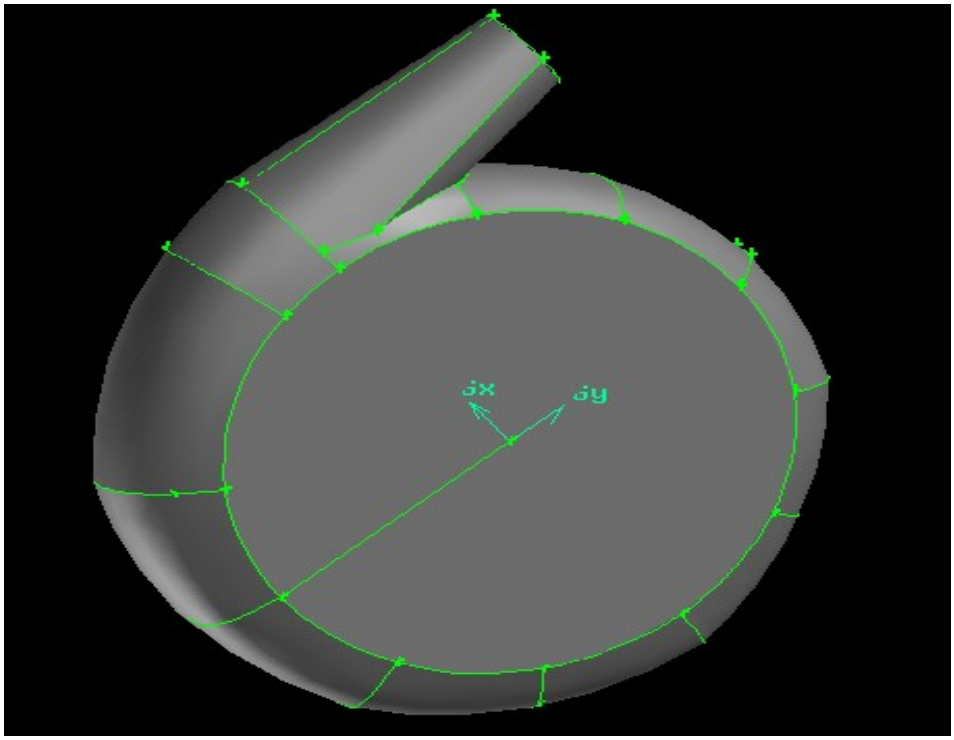

Figure 4.2 Cad model of fluid in casing

Inlet passage

The inlet passage of the centrifugal slurry pump had a complicated structure with several fillets and sections at different angles. For this reason several moulds of different areas were made; from these sections geometry of passage at different locations was obtained. These sections were extended and combined together to model the fluid portion in the inlet passage.

The modeling was done in two different software's Pro-engineer and Gambit. This was because

Pro-Engineer is a modeling software and has sophisticated modeling tools that helped in modeling the complex geometries. Apart from the modeling tools the software has features that helped in creating cross-sections at different locations which helped in better visualization and

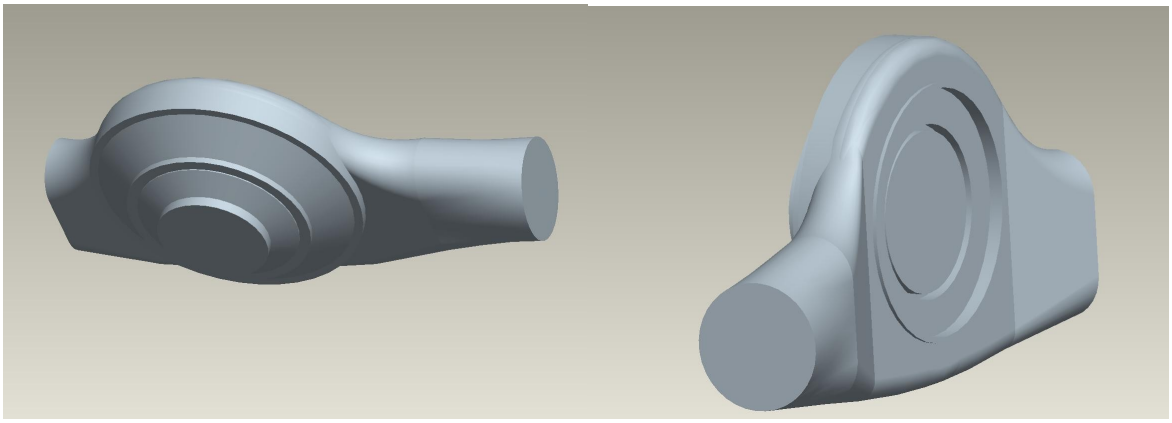

Figure 4.3 CAD model of fluid volume of inlet passage

Understanding of the actual pump geometry .GAMBIT is a pre processor and has powerful tools for meshing and defining the problem for analysis. Since the problem was to be solved in FLUENT .GAMBIT was preferred as it is specifically programmed for defining problems in FLUENT. The meshing tools in GAMBIT help in controlling the mesh of the model. The modeling tools in gambit are more powerful when using bottom up approach in modeling the geometry as it is more flexible and any complicated geometry can be easily modeled if the required data is available.

4.3 PUMP ASSEMBLY

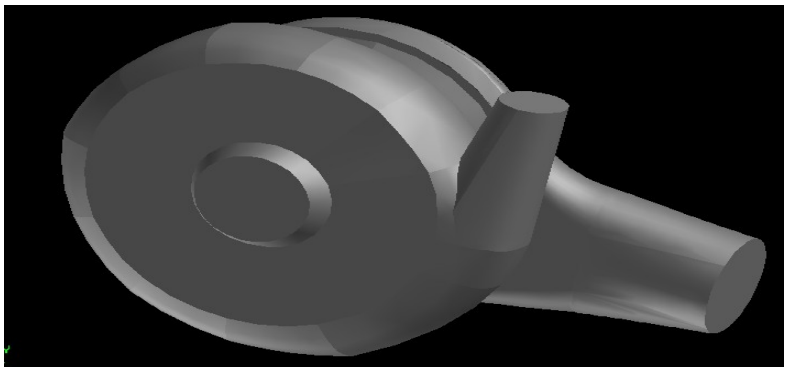

Figure 4.4 Assembly model of pump components

4.4 TYPES OF MESHING SCHEME

- **Edge meshing schemes**
- **Face meshing schemes**
- **Volume meshing schemes**

4.4.1 Edge meshing schemes

- Bi-exponent
- Bell Shaped

Bi-exponent

The Bi-Exponent scheme divides the edge into two segments of equal length and applies the exponent grading scheme separately to each segment.

Bell Shaped

The Bell Shaped scheme grades the edge such that the mesh node density obeys a normal distribution centered at the geometric center of the edge.

4.4.2 Face meshing schemes

Face element type

The Face Element Type specifies the mesh node configuration associated with either of two available face element shapes. To set the face element type the node pattern associated is specified with each of the face element shapes. There are two face element shapes available:

- Quadrilateral
- Triangle

Each face element shape is associated with three different node patterns, and each node pattern is characterized by the number of nodes in the pattern. Figure 5.11 and Figure 5.12 show the node

patterns associated with the quadrilateral and triangular face element types, respectively.

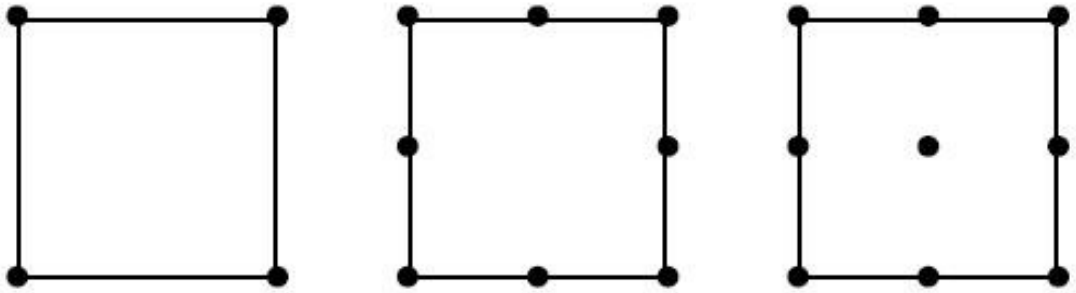

Figure 4.5 Quadrilateral face element types 4, 6 and 8 Node elements

Figure 4.6 Triangular face element types 3 Node and 6 Node elements

When setting a face element type, the pre-processor applies the type to all face elements of the specified shape. For example, to specify 8-node quadrilateral face elements, the pre-processor locates mesh nodes according to the 8-node pattern for all quadrilateral face elements produced in the subsequent face meshing operation.

4.4.3 Volume meshing schemes

Volume Element Type is used to specify the number of mesh nodes and the node pattern associated with any of four available volume element shapes. To set the volume element type,

you must specify the numbers of nodes associated with each of the volume element shapes. There are four volume element shapes available.

- Hexahedron
- Wedge
- Tetrahedron
- Pyramid

Every volume element shape is associated with as many as five different node patterns. Each node pattern is characterized by the number of nodes in the pattern. The node patterns associated with each volume element shape are as follows:

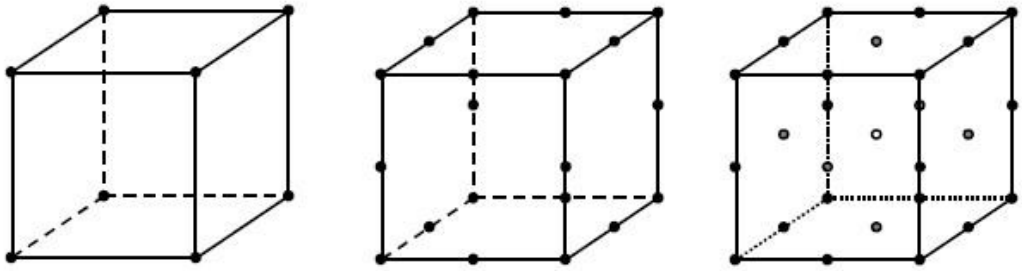

Figure 4.7 Hexahedron volume elements

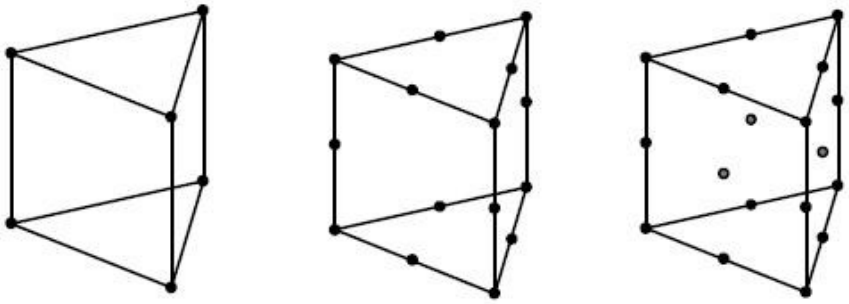

Figure 4.8 Wedge volume elements

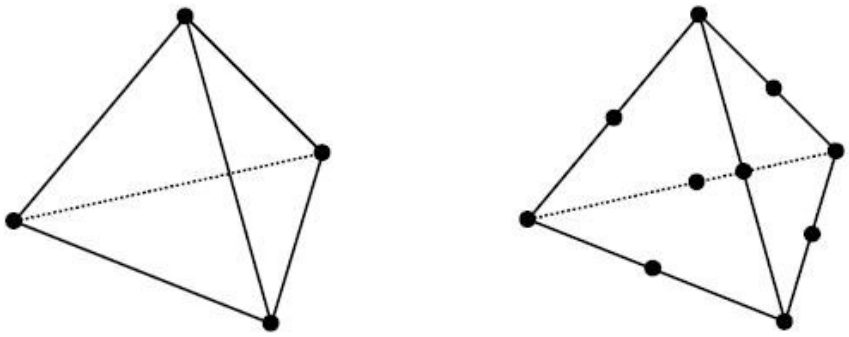

Figure 4.9 Tetrahedron volume elements

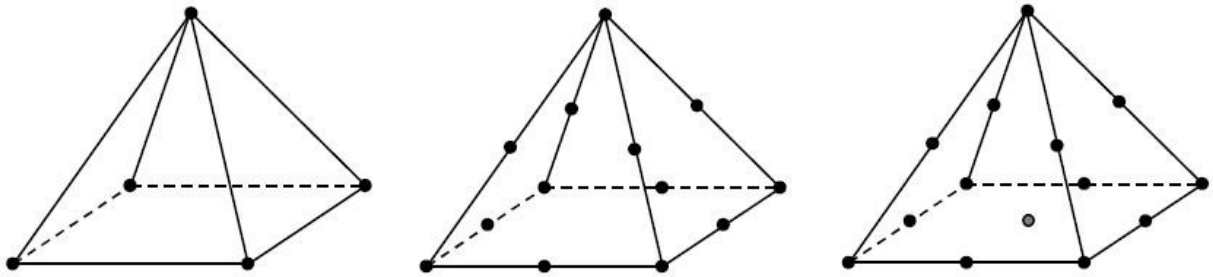

Figure 4.10 Pyramid volume elements

Shape	Numbers of Nodes
Hexahedron	8, 20, 27
Wedge	6, 15, 18
Tetrahedron	4, 10
Pyramid	5, 13, 14

Table 4.1 Element shape and number of nodes

to set a volume element type, the pre-processor applies the specified mesh node pattern to all volume elements of the specified shape. For example, if you specify 20-node wedge volume elements, pre-processor locates mesh nodes according to the 20-node pattern for all wedge volume elements produced in the subsequent volume meshing operation.

4.5 MESHING OF PUMP ASSEMBLY WITH DIFFERENT MESH SIZE

4.4.2 Meshing of pump assembly with grid interval size 6

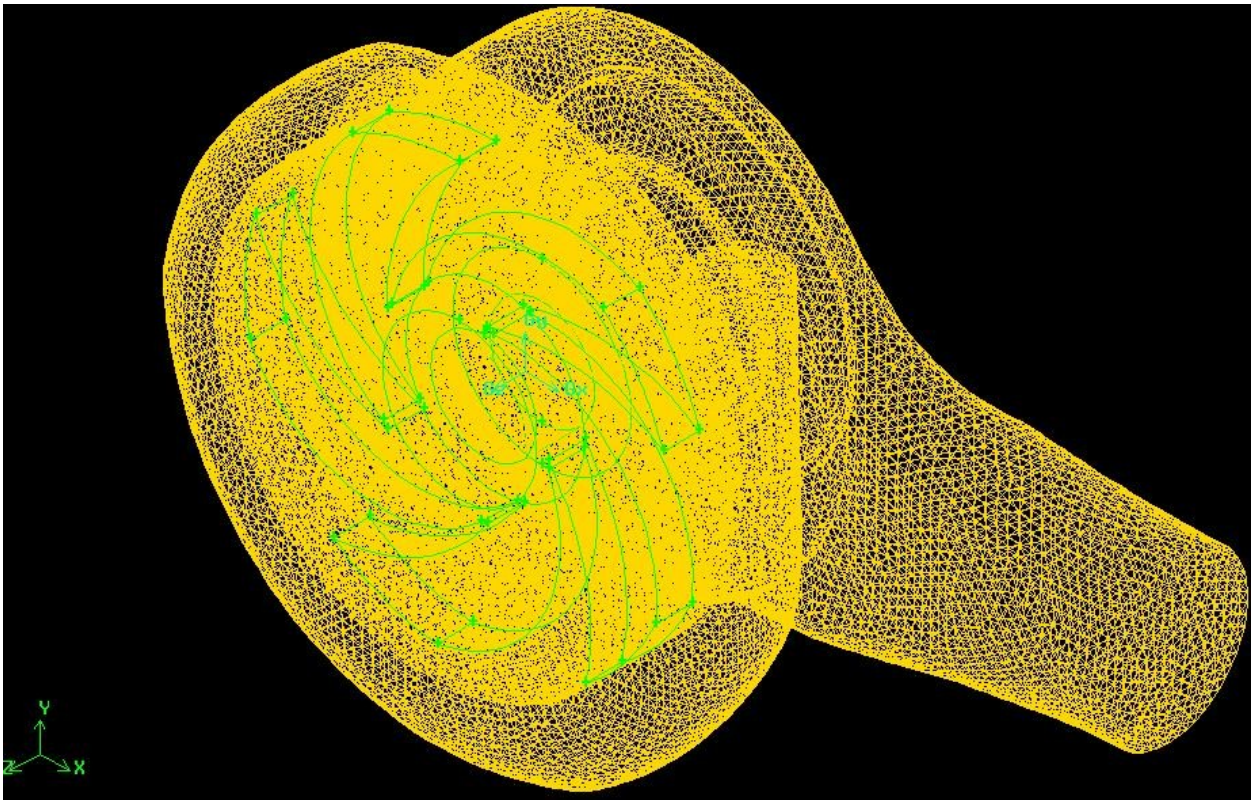

Figure 4.11 Coarse mesh (tetrahedral elements with interval count 6)

Table 4.2 Number of elements in different mesh volumes

Volume	No of elements
Fluid in impeller	30760
Inlet passage(4 highly skewed elements)	116026
Casing	110149

4.4.2 Meshing of pump assembly with grid interval size 5

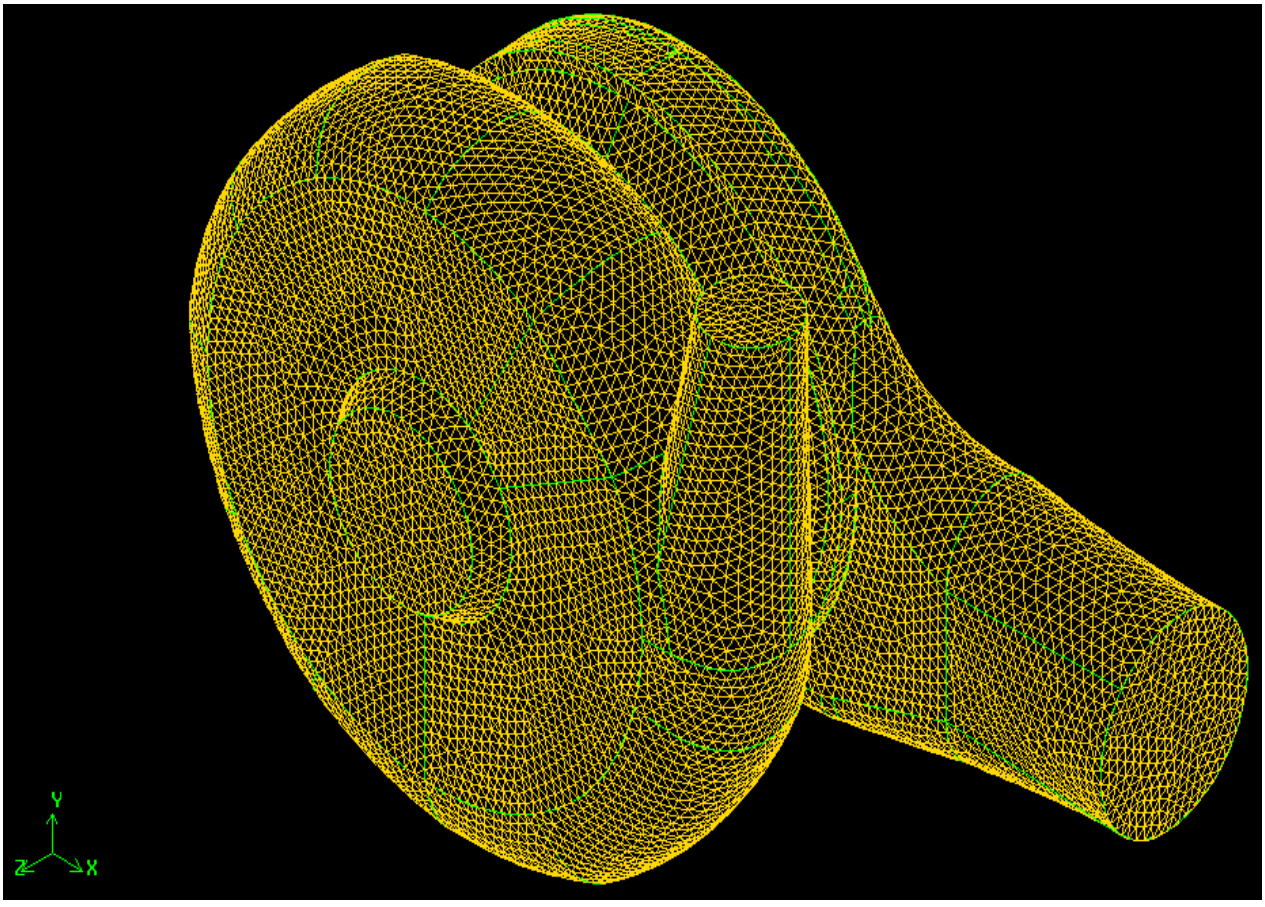

Figure 4.12 Mesh (tetrahederal elements with interval count 5)

Table 4.3 No of elements in different mesh volumes

Volume	No of elements
Fluid in impeller	91736
Inlet passage(2 highly skewed elements)	247462
Casing	334676

4.4.3 Meshing of pump assembly with grid interval size 3

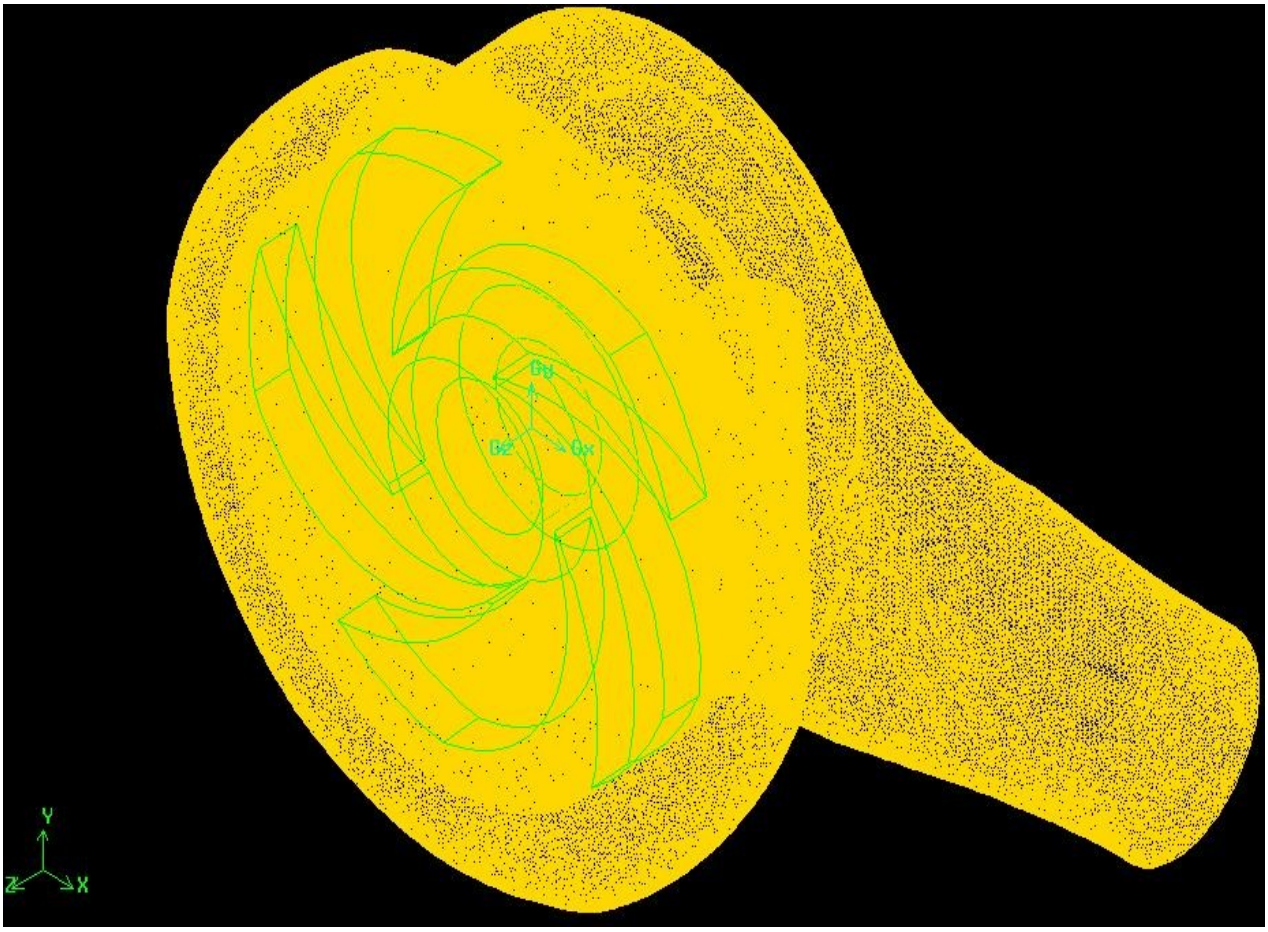

Figure 4.13 Fine mesh (tetrahedral elements with interval count 3)

Table 4.4 No of elements in different mesh volumes

Volume	No of elements
Fluid in impeller	153730
Inlet passage(2 highly skewed elements)	733536
Casing	739357

CHAPTER 5

COMPUTATIONAL EVALUATION OF PUMP PERFORMANCE

5.1 SIMULATION OF PUMP

After meshing of the model of pump assembly commercial CFD code FLUENT is used for simulation of the pump performance .The boundary conditions of mass flow rate given at pump inlet. The performance results are obtained at different mass flow rate conditions with constant operating speed by taking different turbulent modeling. Numerical performance results compared with the experimental results at the same operating conditions.

5.1.1 Assumptions

The following assumptions were taken for simulation:

- The walls of the casing were assumed to be smooth hence any disturbances in flow due to roughness of the surface were neglected.
- The friction co-efficient for all surfaces were set to 0, hence friction between the walls and fluid was neglected.
- Steady state conditions and incompressible fluid flow.

5.1.2 Solution parameters

- 3-D double precision solver used to solve for simulation
- Multiple reference frame technique used to simulate the pump performance
- Clear water used is taken as working fluid
- Standard K-Epsilon , K-omega, Eddy large simulation model are used for turbulence modeling.
- Convergence criteria for continuity, velocity and turbulence parameters was set to 10^{-3}
- Second order scheme is used for pressure correction as well as for solving momentum, turbulent kinetic energy and turbulence dissipation rate.
- simple scheme is used for pressure velocity coupling

5.2 PRESSURE AND VELOCITY DISTRIBUTION OF IMPELLER AND CASING.

5.2.1 Pressure and velocity distribution of impeller at 1450 rpm.

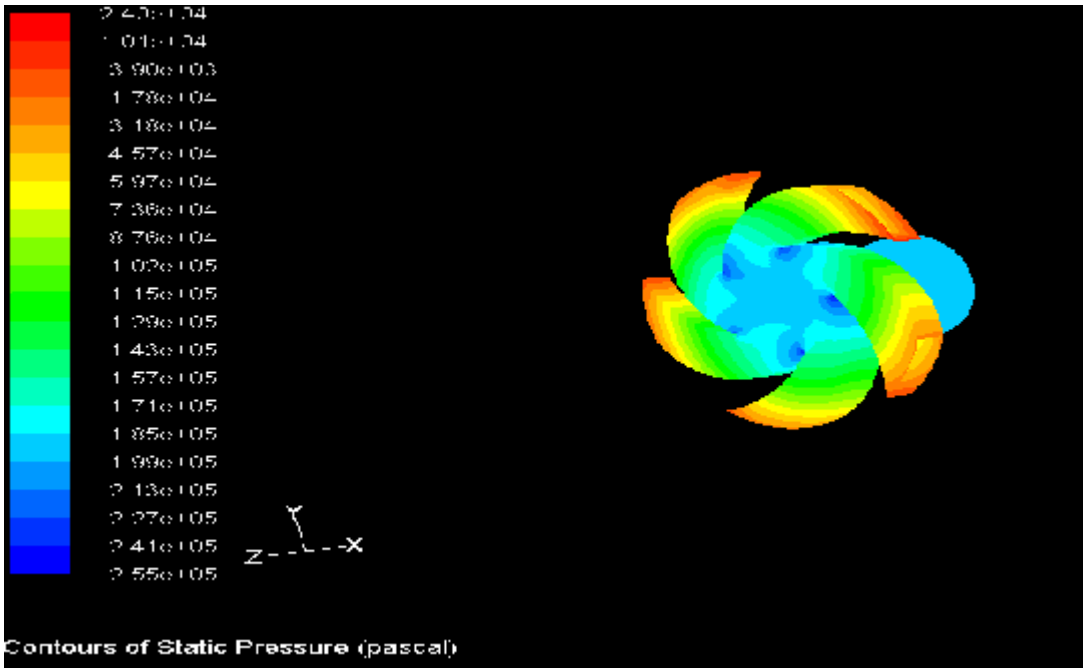

Figure 5.1 Pressure distribution of impeller at 1450 rpm

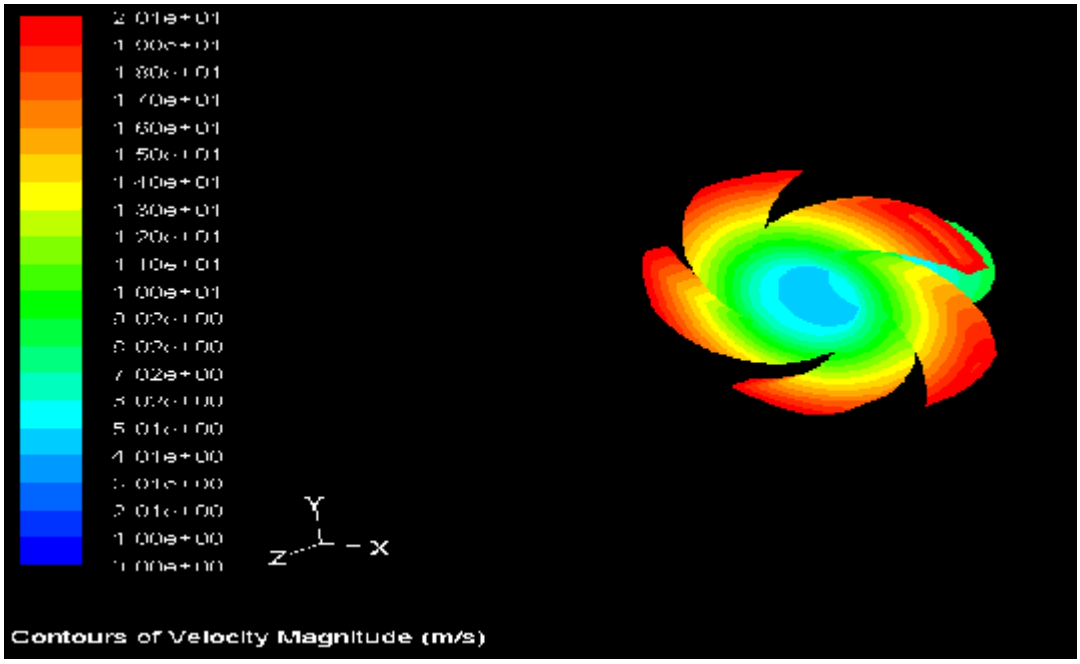

Figure 5.2 velocity distribution of impeller at 1450 rpm.

5.2.3Pressure and velocity contour of impeller at 1200 rpm.

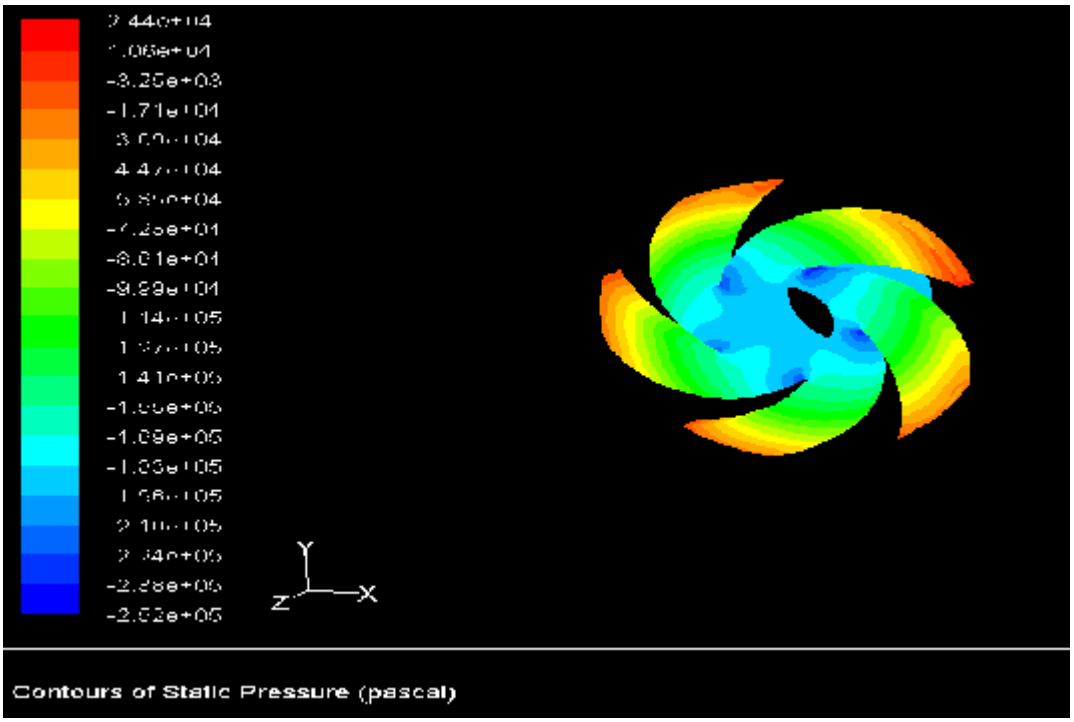

Figure 5.3 Pressure distribution of impeller at 1200 rpm

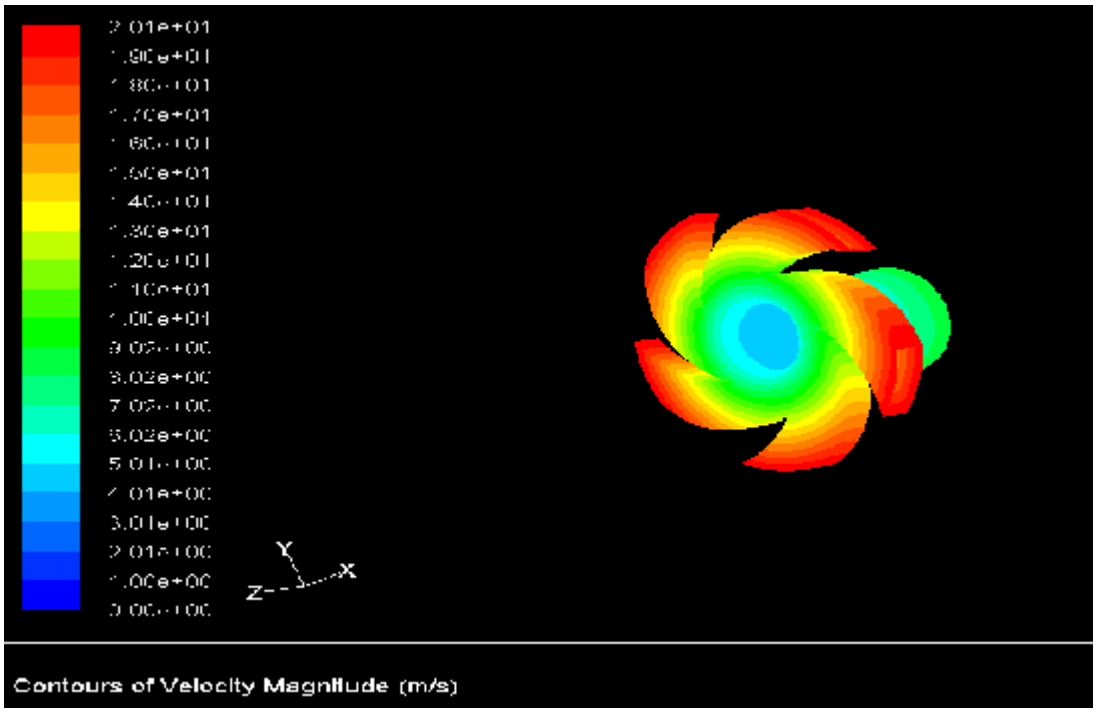

Figure 5.4 Velocity distribution of impeller at 1200 rpm

5.2.3Pressure and velocity contour of impeller at 1000 rpm.

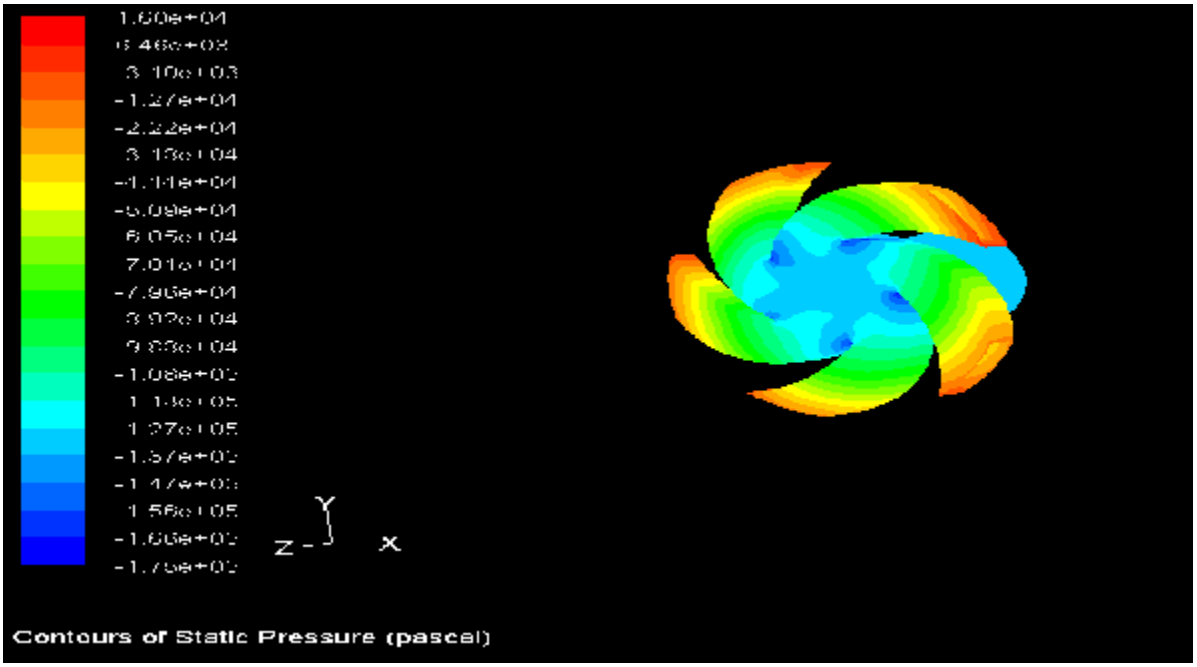

Figure 5.5 Pressure distribution of impeller at 1000 rpm

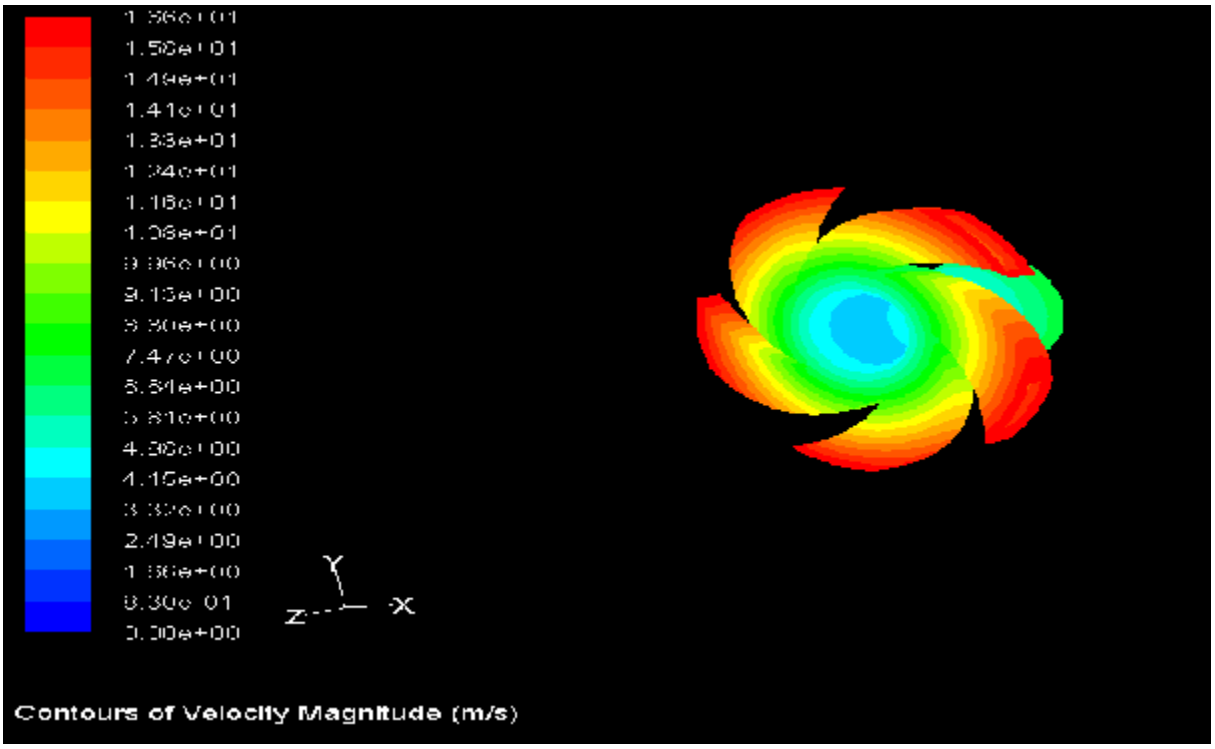

Figure 5.6 velocity distribution of impeller at 1000rpm

5.2.4 Pressure and velocity contour of impeller at 800 rpm.

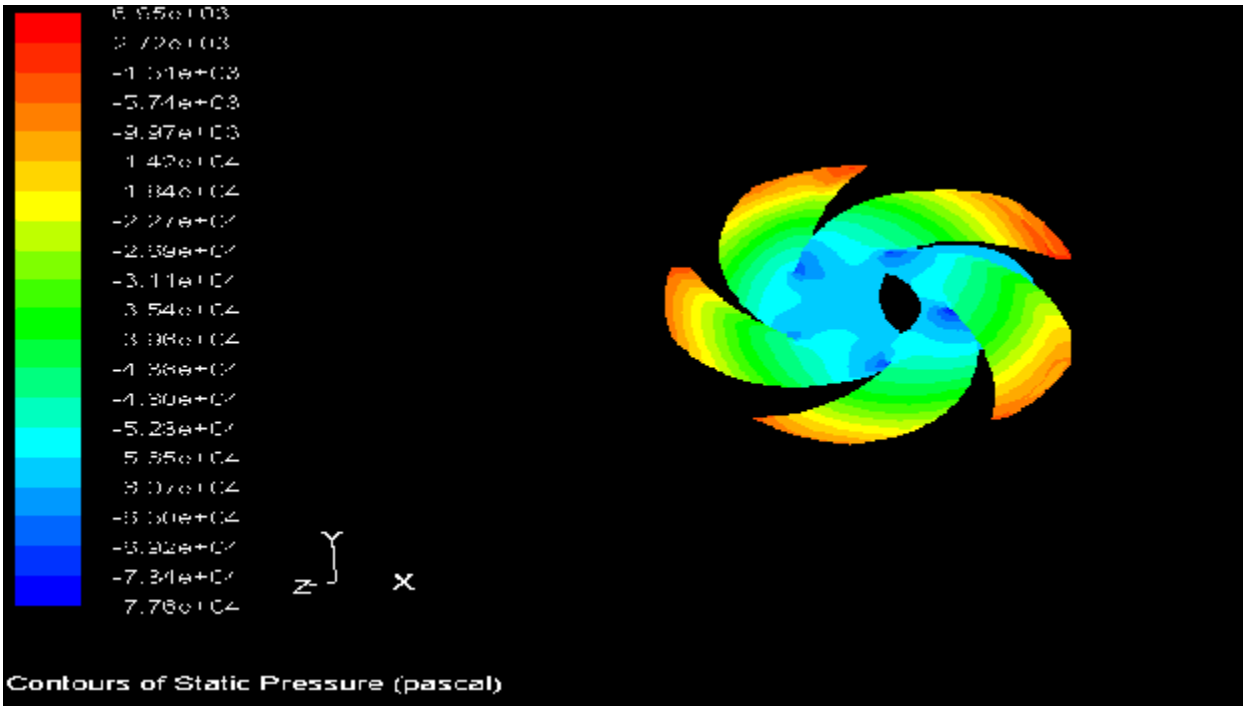

Figure 5.7 Pressure distribution of impeller at 800

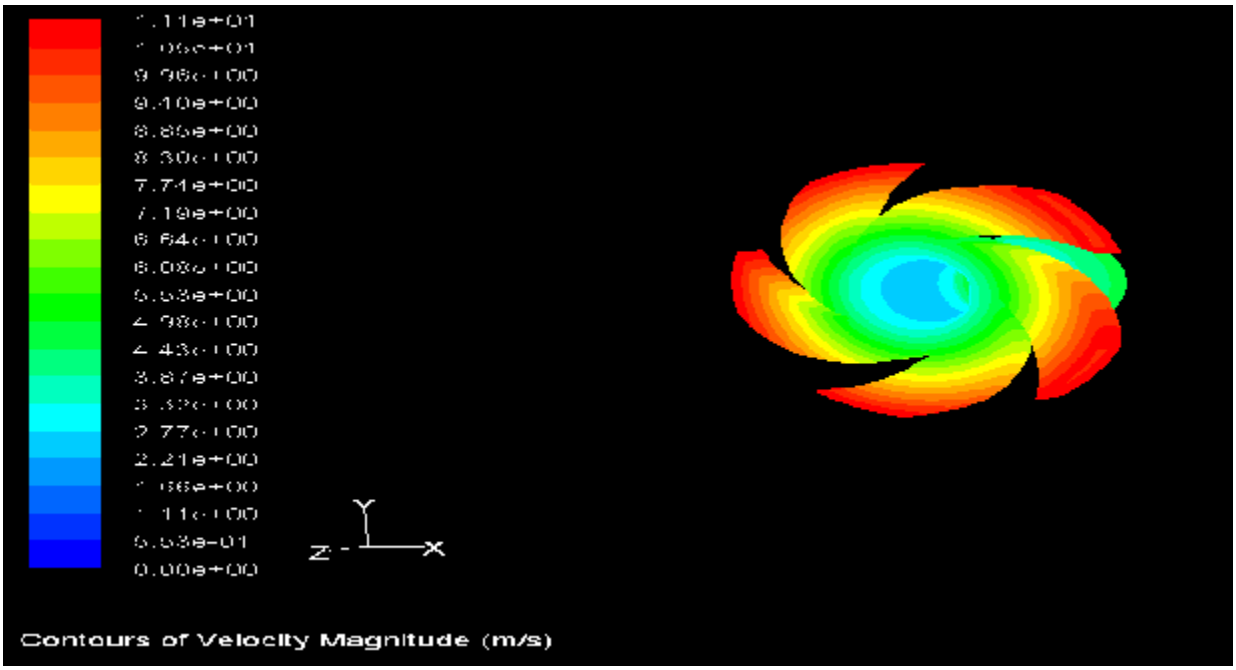

Figure 5.8 velocity distribution of impeller at 800 rpm

5.2.5 Pressure and velocity contour of casing at 1450 rpm.

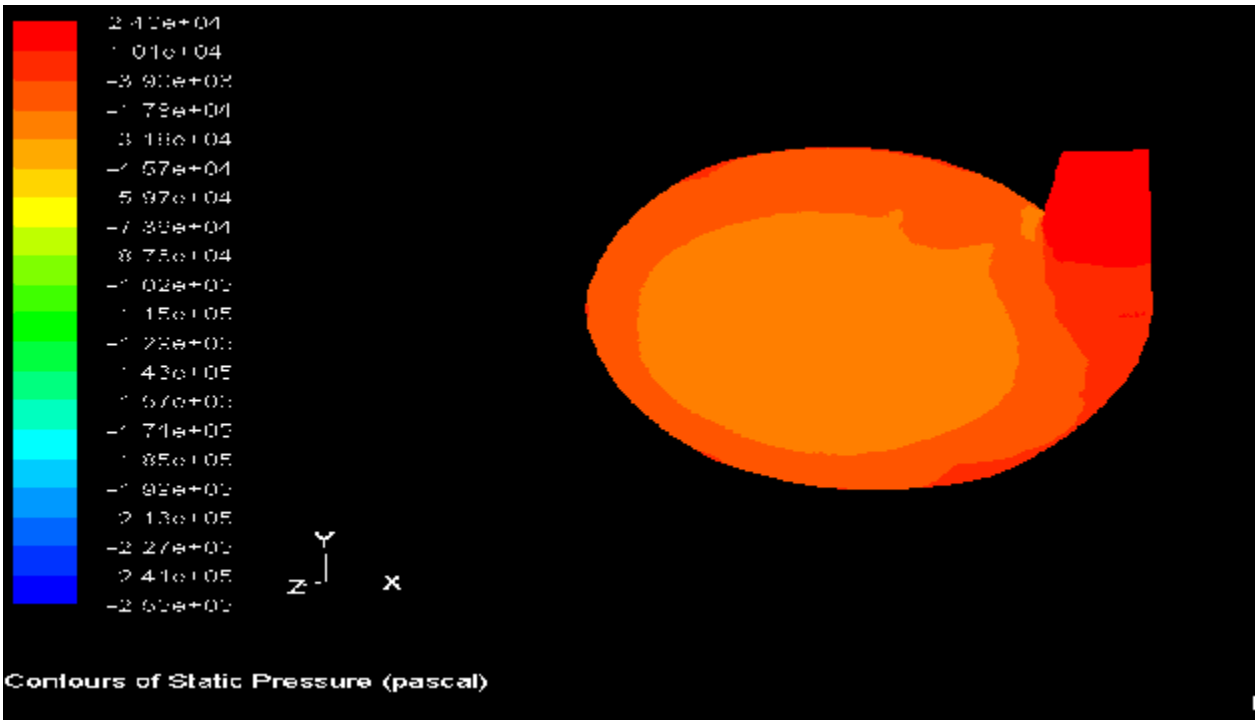

Figure 5.9 Pressure contour of casing

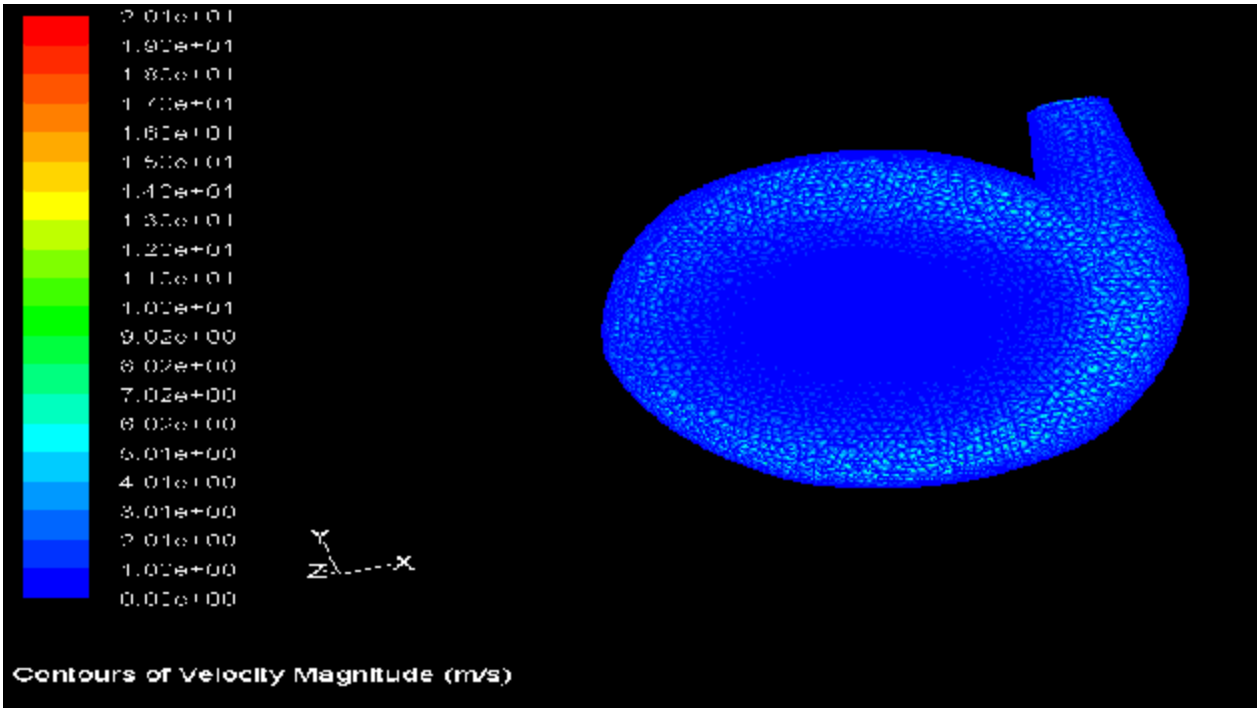

Figure 5.10 Velocity contour of casing

5.2.6 Pressure and velocity contour of casing at 1200 rpm.

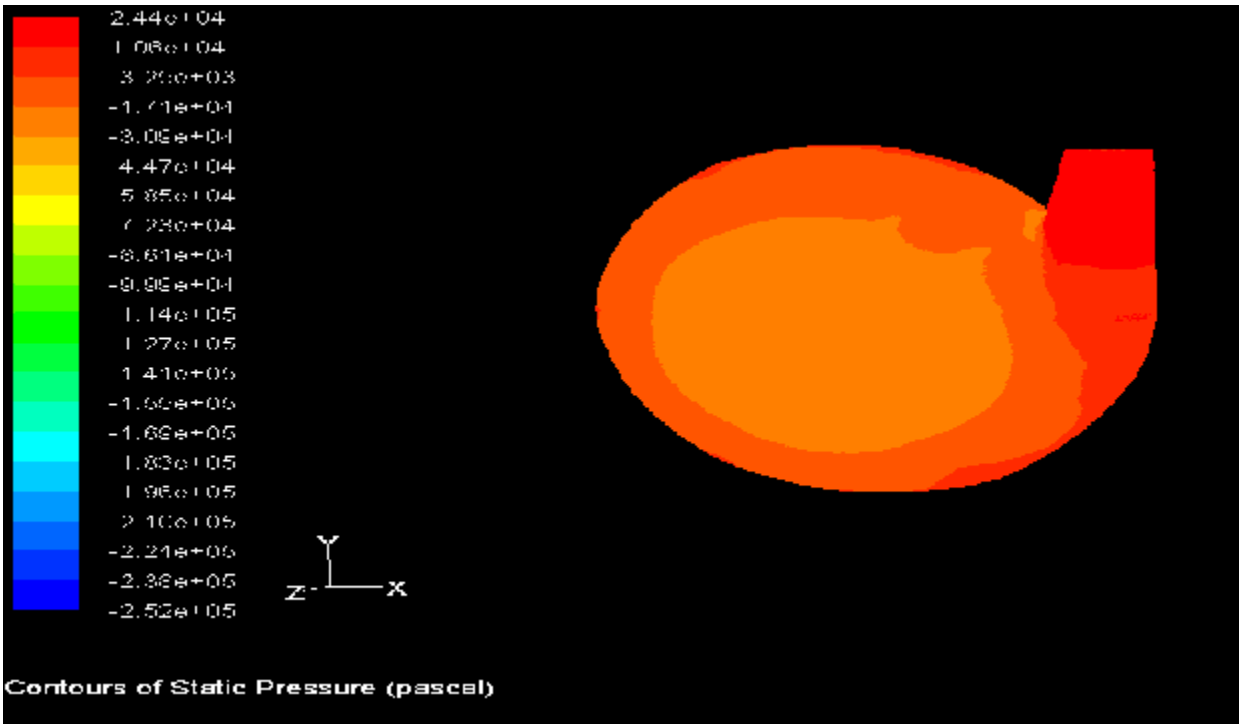

Figure 5.11 Pressure contour of casing

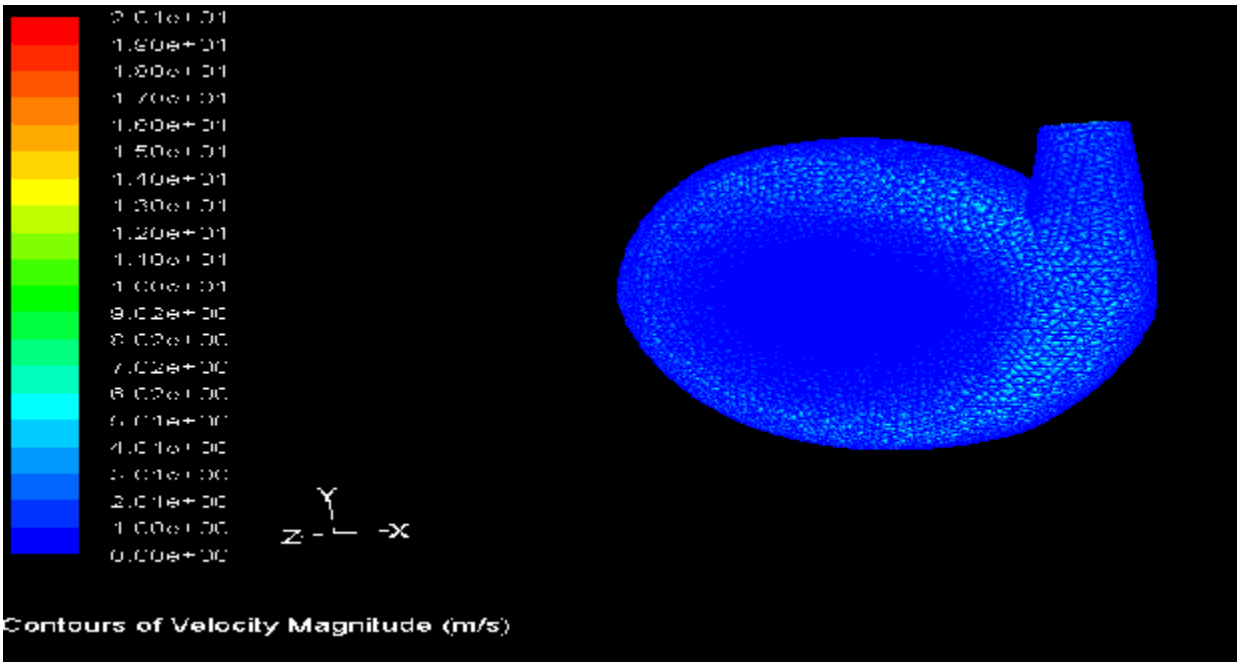

Figure 5.12 Velocity contour of casing

5.2.7 Pressure and velocity contour of casing at 1000 rpm.

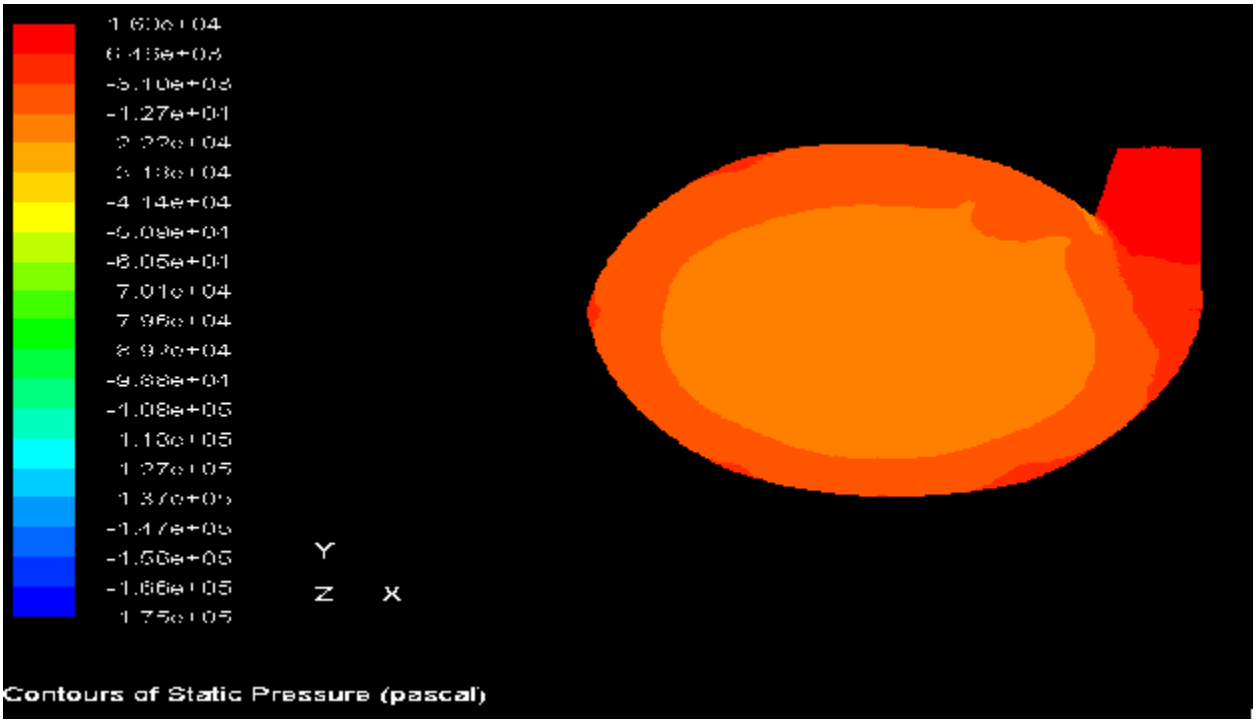

Figure 5.13 Pressure contour of casing

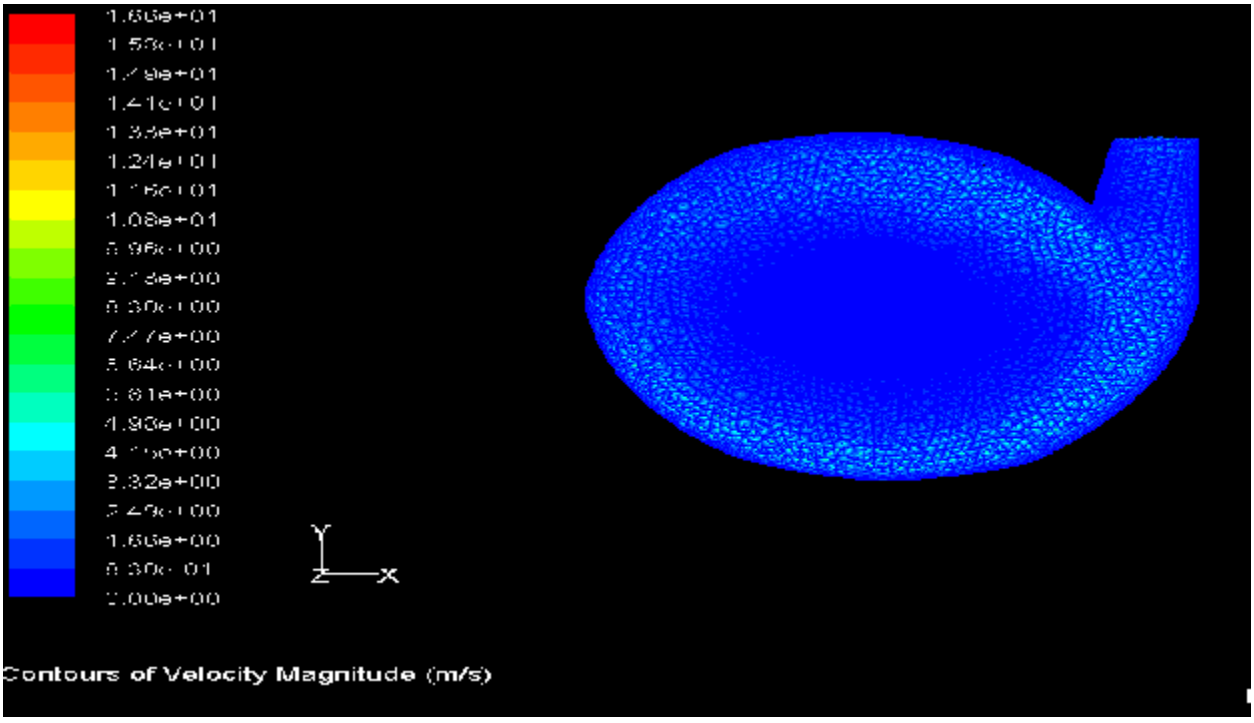

Figure 5.14 Velocity contour of casing

5.2.8 Pressure and velocity contour of casing at 800 rpm.

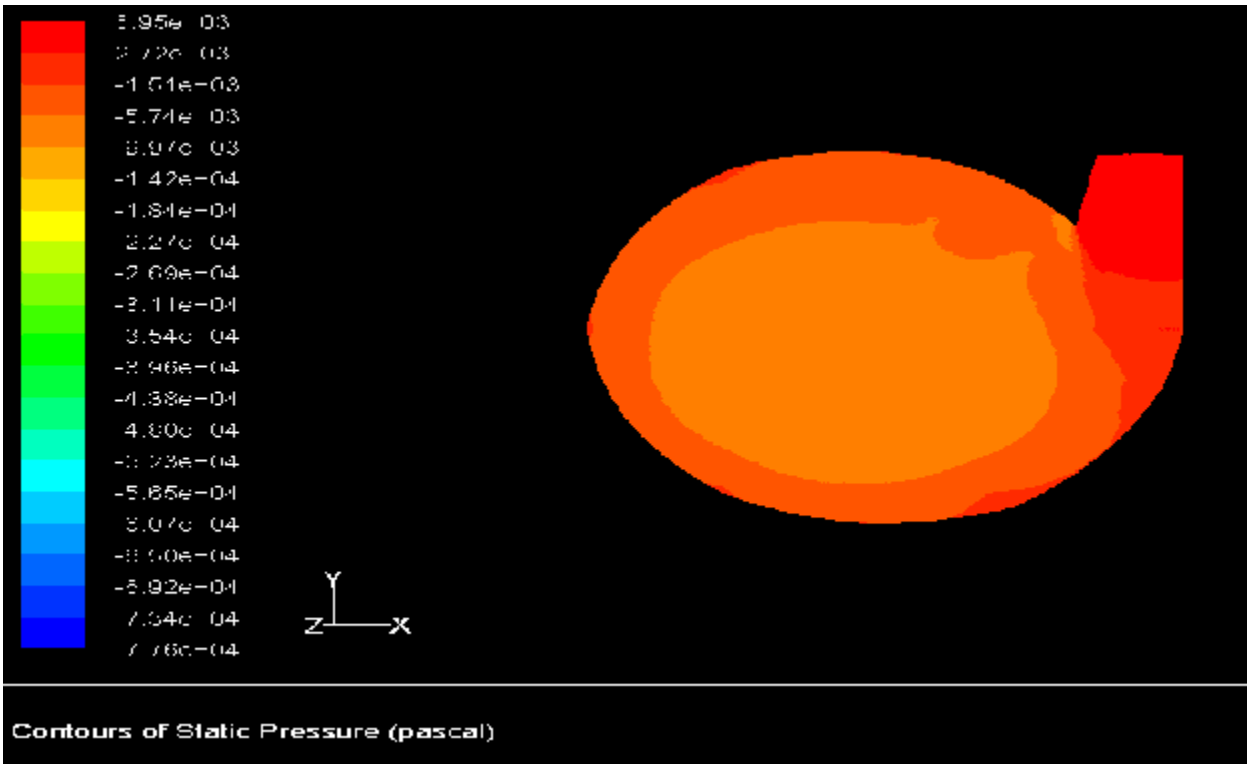

Figure 5.15 Pressure contour of casing

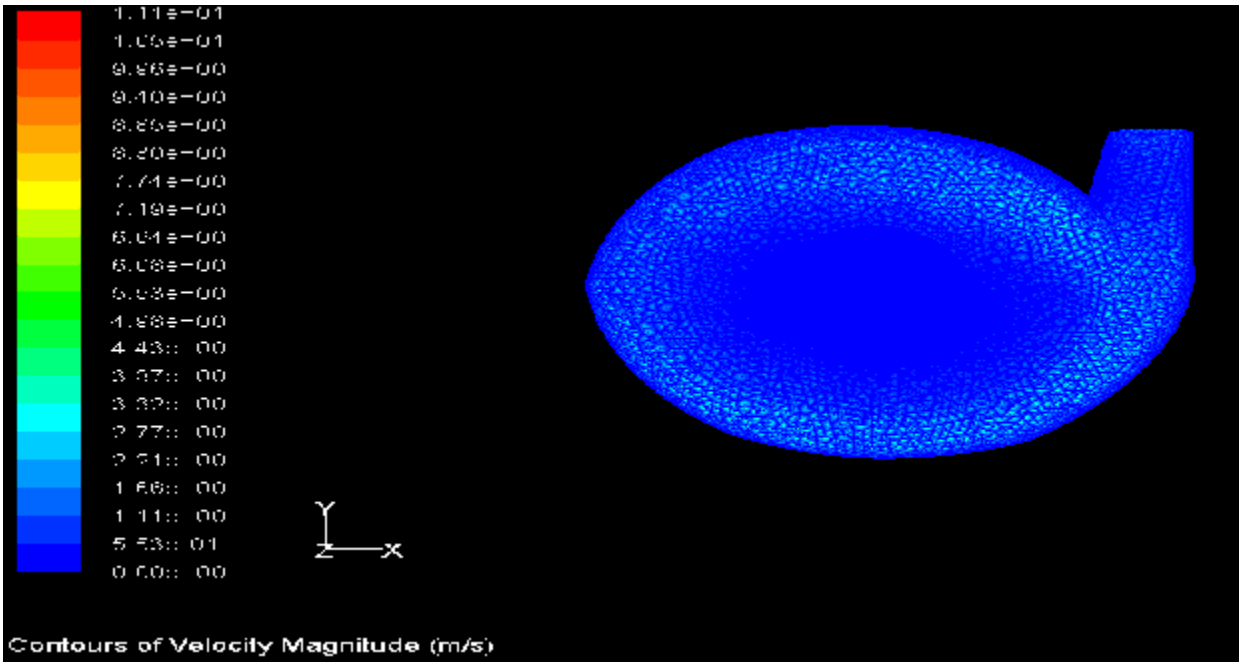

Figure 5.16 Velocity contour of casing

5.2.9 Velocity vector of impeller and casing

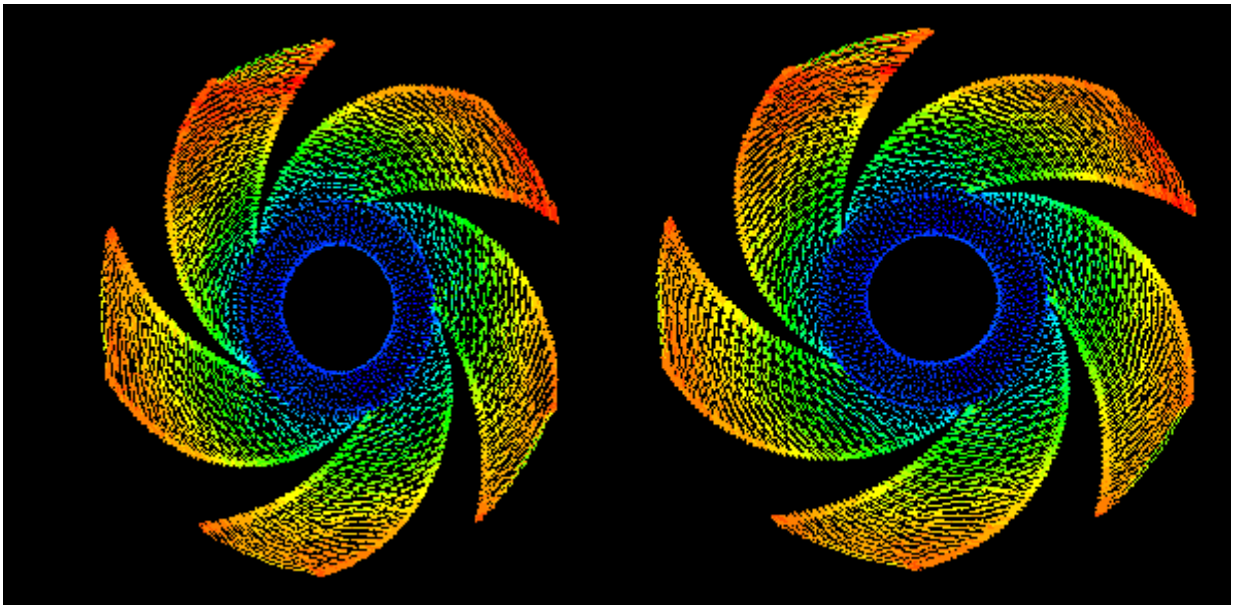

Figure 5.17 velocity vector of impeller

Figure 5.18 velocity vector of impeller

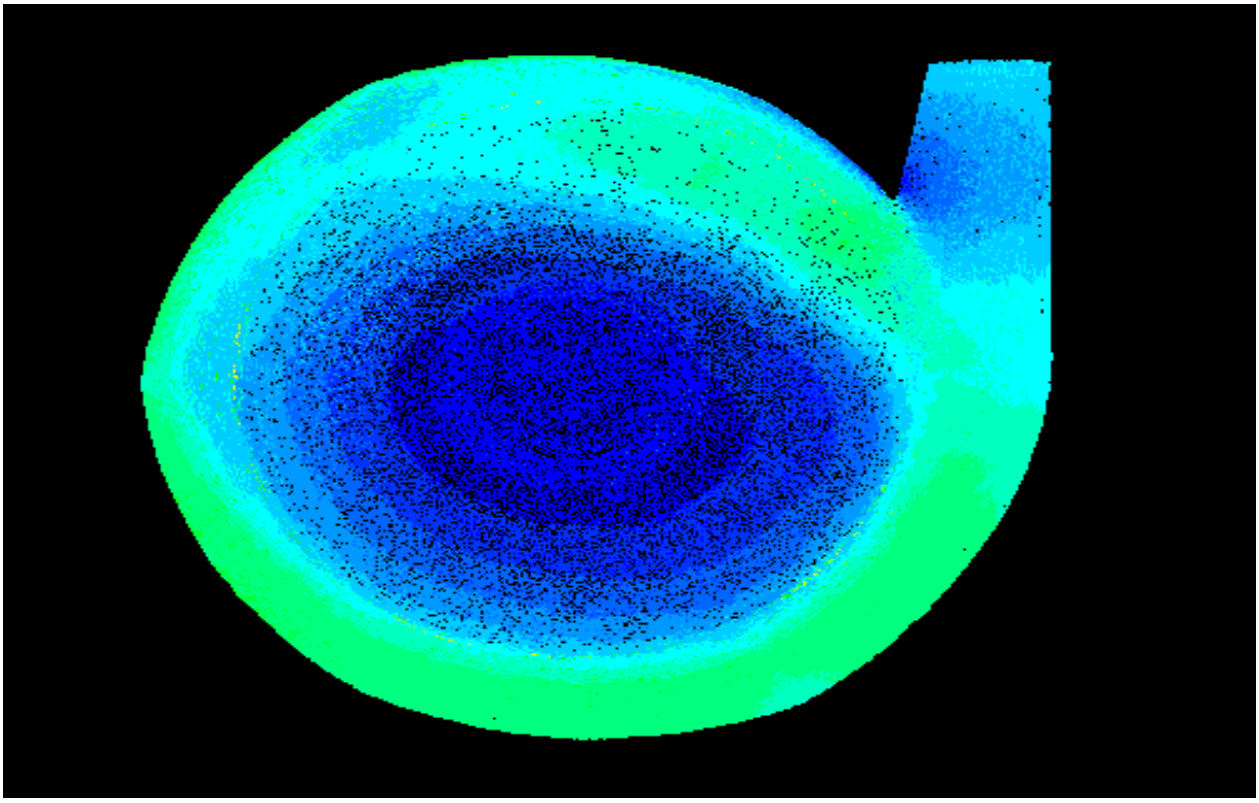

Figure 5.19 velocity vector of casing

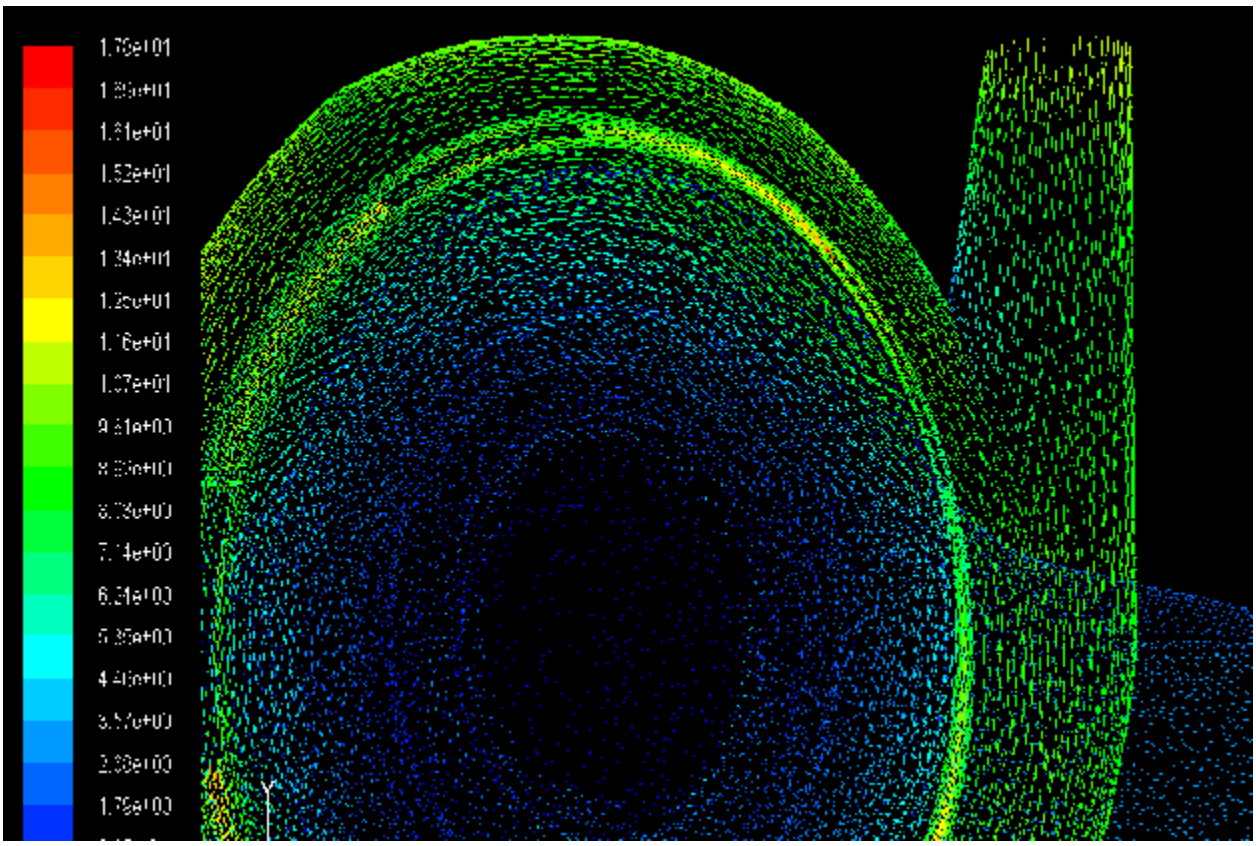

Figure 5.20 velocity vector of pump without impeller

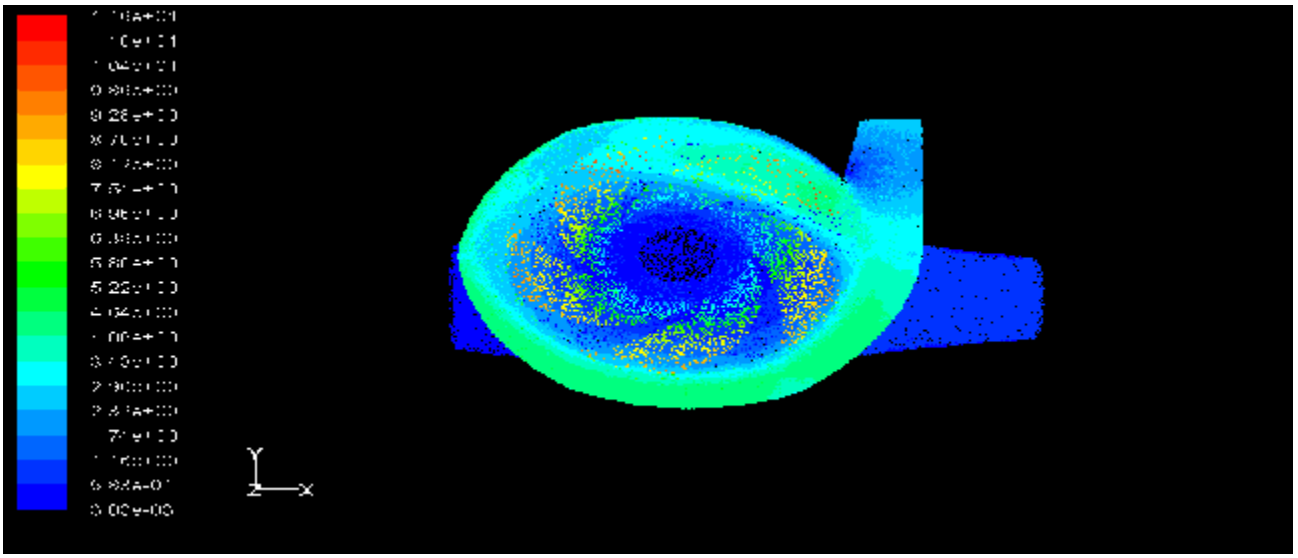

5.21 Velocity vector in complete pump

Velocity vectors: - Velocity vectors may be help to identify directional motion of fluid particles in impeller domain. It can be seen internal circulation and separation zones in impeller vane channels in figure 5.19-5.21

5.3 PERFORMACE CHARACTERSTIC OF PUMP

The performance characteristic of the centrifugal slurry pump has been predicted numerically handling clear water. Head, power and efficiency characteristics of the pump are predicted by CFD analysis at 1450 rpm, 1250 rpm and 1000 rpm and 800 rpm explained graphically in Figures 5.22-5.25. The Numerical results on pump performance handling clear water using three different turbulent modelling namely as K-Ebsilen ,K-Omega and Eddy Large Simulation at the different rated speed of 1450,1200,1000,800 rpm are given in Table 5.1-5.4 The parameters namely discharge rate, total head, input power and efficiency are tabulated for a constant pump speed of 1450 rpm.

Table 5.1 Result of pump performance by experimental and simulation at 1450 rpm.

Sr. No	Discharge Q (lps)	Head (m) Experimental	Simulation (k-€)	Simulation (k-w)	Simulation (ELS)
1	10.75	11.66	12.5563	12.7	12.4
2	9.591	12.60	13.4623	13.6235	13.3025
3	8.71	13.32	14.5636	14.7256	14.4023
4	7.633	14.21	15.236	15.4	15.1023
5	5.935	15.09	15.9236	16.12	15.8023
6	4.375	15.54	16.3956	16.5236	16.2365
7	2.876	16.01	16.8563	16.95365	16.7123
8	1.204	16.42	17.1986	17.2963	17.07
9	0	16.60	17.3654	17.4823	17.22

Table 5.2 Result of pump performance by experimental and simulation at 1200 rpm.

Sr. No	Discharge Q (lps)	Head (m) Experimental	Simulation (k-€)	Simulation (k-w)	Simulation (ELS)
1	8.71	7.93	8.7563	8.8563	8.6523
2	7.57	8.5	9.4568	9.6023	9.3023
3	6.69	9.04	9.9236	10.023	9.8232
4	5.32	9.70	10.5698	10.685	10.4532
5	4.50	10.14	10.9236	11.02	10.82365
6	3.44	10.50	11.3698	11.4632	11.263
7	2.29	10.82	11.8089	11.92	11.7123
8	1.18	11.06	11.8793	11.9765	11.7765
9	0	11.51	12.1652	12.263	12.0236

Table 5.3 Result of pump performance by experimental and simulation at 1000 rpm.

Sr. No	Discharge Q (lps)	Head (m) Experimental	Simulation (k-€)	Simulation (k-w)	Simulation (ELS)
1	7.051	5.448843	6.3969	6.5	6.236
2	6.135	5.857321	6.807	6.907	6.72
3	5.552	6.168565	7.1625	7.2633	7.023
4	4.778	6.52157	7.5236	7.6236	7.3596
5	3.573	6.959297	7.936	8.036	7.8236
6	2.664	7.278147	8.2978	8.396	8.02365
7	1.658	7.495039	8.5023	8.6123	8.3256
8	0.95	7.58002	8.56	8.6632	8.4365
9	0	7.661239	8.66	8.76	8.52

Table 5.4 Result of pump performance by experimental and simulation at 800 rpm.

Sr. No	Discharge Q (lps)	Head (m) Experimental	Simulation (k-€)	Simulation (k-w)	Simulation (ELS)
1	5.384	3.484436	4.5623	4.7032	4.4563
2	4.742	3.7779761	4.8623	4.96235	4.7632
3	3.995	3.9732178	5.02645	5.1836	4.9285
4	3.785	4.0389916	5.13256	5.2436	4.966
5	2.724	4.3392764	5.4023	5.50632	5.2536
6	2.261	4.5022703	5.60345	5.7236	5.4523
7	1.536	4.659495	5.76365	5.869	5.6632
8	0.886	4.7340406	5.8423	5.9236	5.7456
9	0	4.8148242	5.8852	5.99	5.756

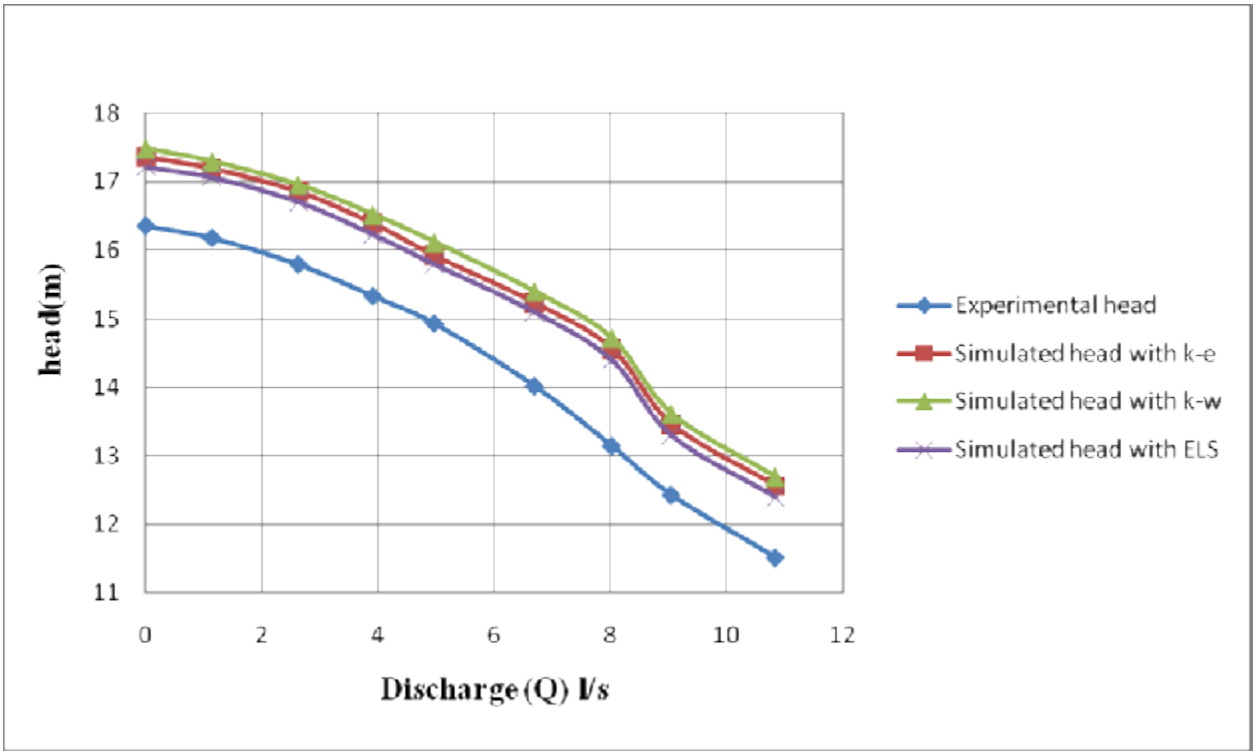

Figure 5.22 Head- Discharge comparisons of pump at 1450 with different turbulent modeling

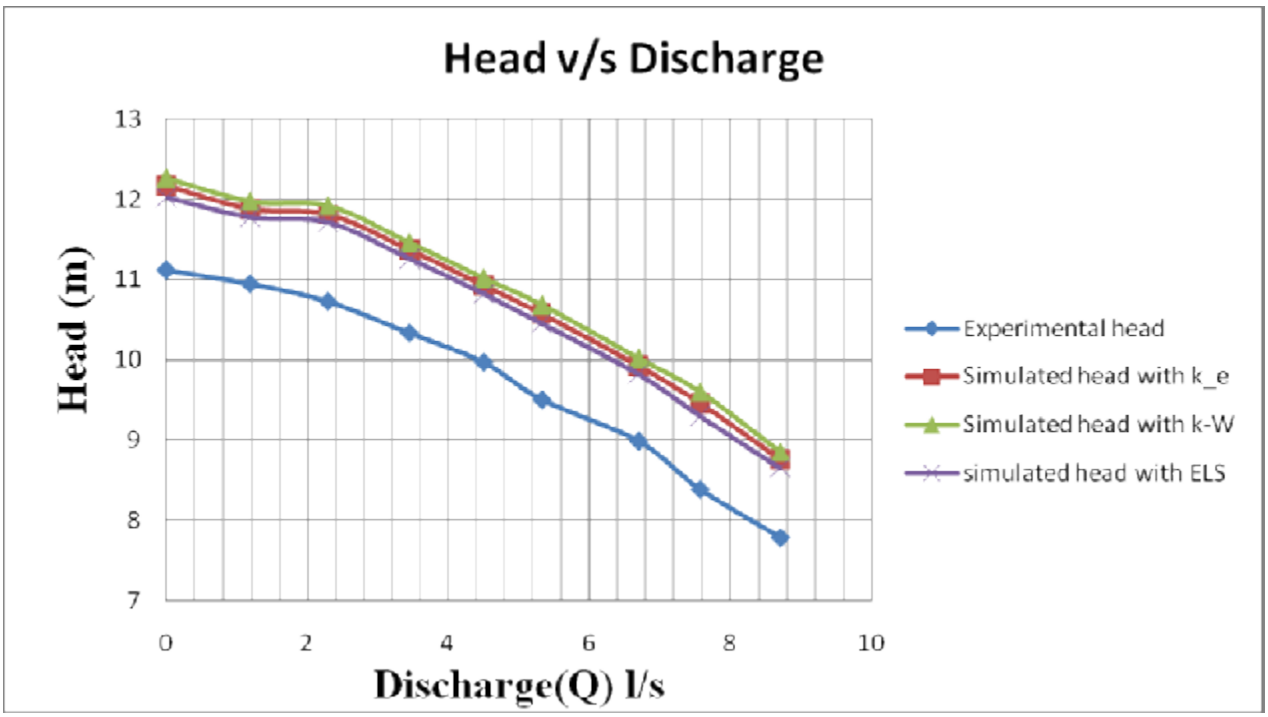

Figure 5.23 Head- Discharge comparisons of pump at 1200 with different turbulent modeling

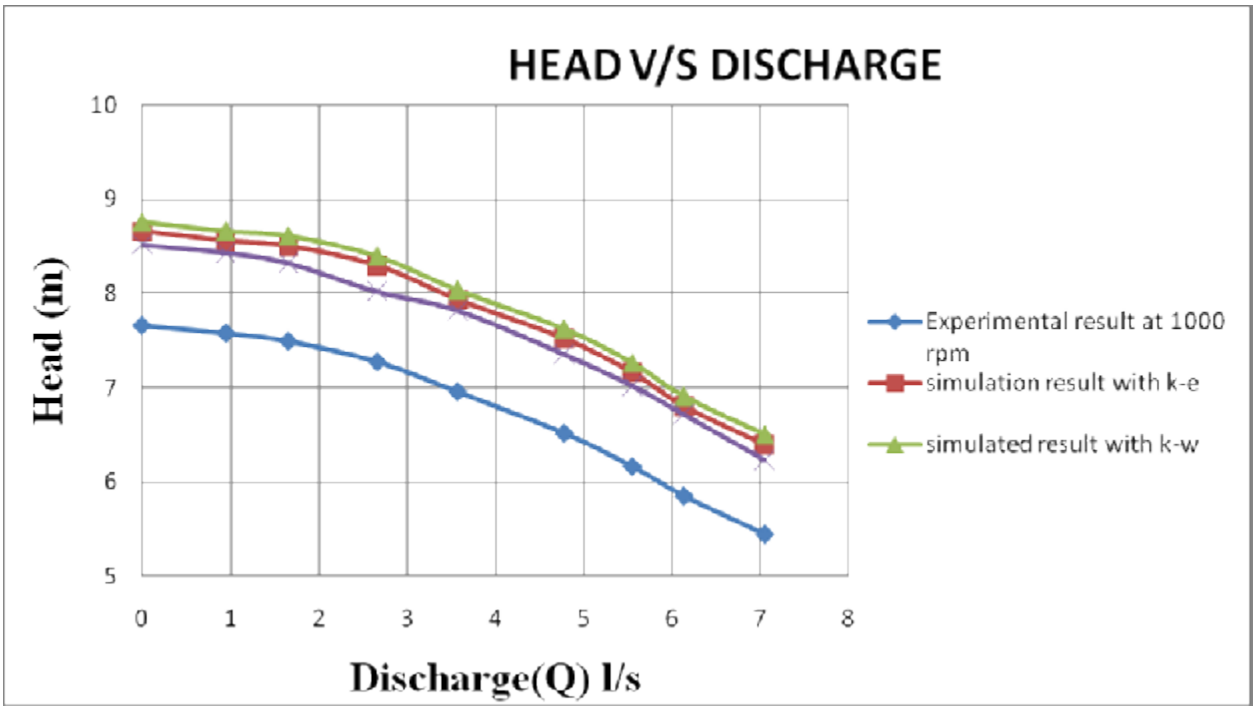

Figure 5.24 Head- Discharge comparisons of pump at 1000 rpm with different turbulent modeling

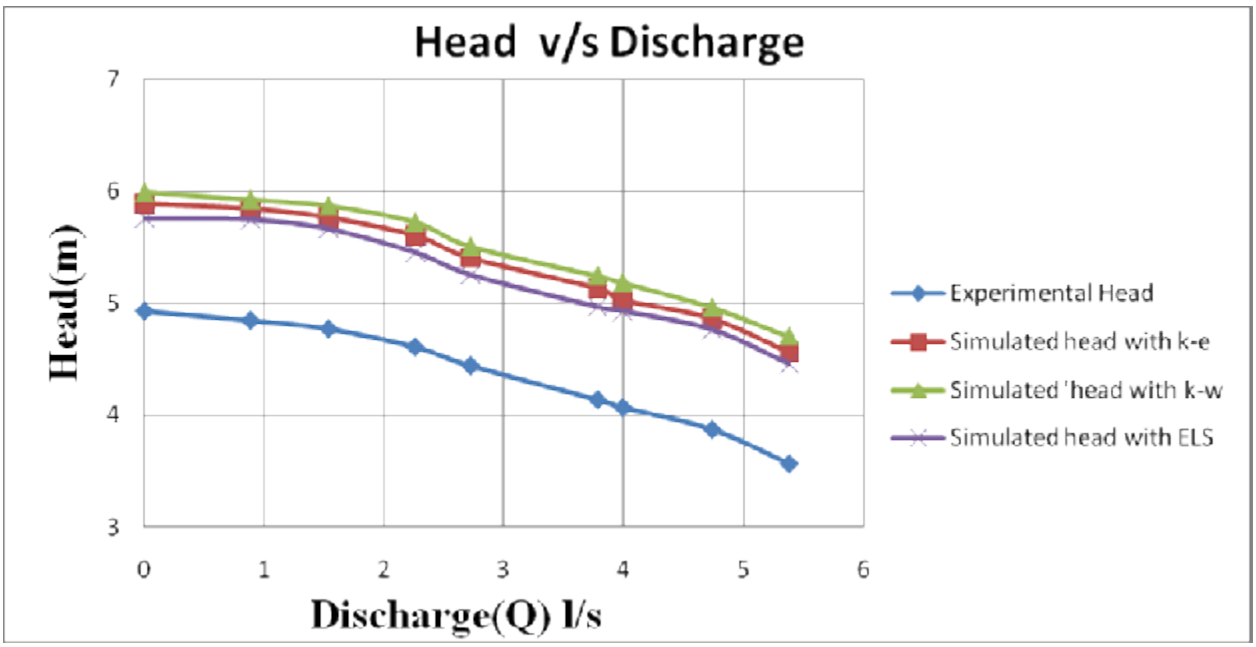

Figure 5.25 Head- Discharge comparisons of pump at 800 rpm with different turbulent modeling

CHAPTER 6

CONCLUSION AND FUTURE WORK

The geometry of pump components impeller, casing, inlet passage, and frame and follower plate is modeled using GAMBIT and PRO-E. The mesh is generated successfully using GAMBIT. Complex internal flow field, pressure and velocity distribution investigated using FLUENT commercial computational code. The simulation results are obtained at the operating speed 1450, 1200, 1000,800 rpm with different mass flow rates for transportation of clear liquid. The Simulation was performed by using different types of turbulent modeling such as k-Epsilon, K-Omega, Eddy large simulation The performance results show that total static head is the function of the mass flow rate with constant operating speed. Numerical performance results of different turbulent modeling are compared with the experimental results at the same operating conditions.

Future Scope

1. Pressure and velocity distribution for pump impeller and casing can be calculated for fly ash slurry.
2. Numerical simulation of centrifugal slurry pump can be evaluated by considering losses.
3. Similar computational simulation models can also be used for analyzing the pressure, velocity and stress distribution of the turbines, compressor, fan and blower.

REFERENCES

1. S.Yedidiah, ”A New Toll for Solving Problems Encountered with Centrifugal Pumps” April 1996 world Pumps Elsevier science.

2. Miner, S. M., “3-D Viscous Flow Analysis of an Axial Flow Pump Impeller” *International Journal of Rotating Machinery*, 1997, Volume 3, No. 3, pp 153-161

3. Murugan, D. M., Tabakoff, W. and Hamed, A., (1997), “Flow Measurements and Flow Analysis in the Exit Region of a Radial Turbine” *International Journal of tating Machines*”, Volume 3, No. 2, pp 93-105.

4. Oh and M.K. Chung (1999), “Optimum values of design variables versus specific speed for centrifugal pumps*”. Proceedings Institution of Mechanical Engineers*, 1999, Vol. 213

5. Majidi, K. and Siekmann H. E., (2000), “Numerical calculation of secondary flow in pump volute and circular casings using 3D viscous flow techniques” International *Journal of Rotating Machinery*, Volume 6, No. 4, pp 245-252

6. Ogut, A. and Pastor, D. G., “Simulation of flow in turbopump vaneless and vaned diffusers with fluid section” *International Journal of Rotating Machinery*, 2000, Volume 6, No. 1, pp 57-65.

7. J.J More, A.B. Palazzolo., Rotodynamic force prediction of whirling centrifugal impeller shroud passages using CFD technique, *Journal of Korea Australia Rheology*, Vol 13, 2001, pp 47-54.

8. Oh and Kim, “Conceptual Design, Optimization of mixed-flow pump impellers using mean streamline analysis”. *Proceedings of Institution of Mechanical Engineers*, 2001, Vol. 215.

9. Wen Guang LI, Flow of viscous oil in the volute of centrifugal pump, *Journal of thermal science*, Vol 11, 2001.

10. Jose. Gonzalez., Carlos. Santolaria., Numerical simulation of dynamic effect due to the impeller volute interaction in a centrifugal pump*, Journal of ASME*, vol 124, 2002.

11. Akira. Goto, Takaki. Sakurai., Hydrodynamic design system for pumps based on 3-D CAD, CFD, and inverse design method, *Journal of ASME*, vol 124, 2002

12. B.K Gandhi, S.N. Singh, V. Seshadri, "Effect of Speed on the Performance Characteristics of a Centrifugal Slurry Pump", *Journal of fluid Engineering*, February, 2002.

13. Kato, C., Mukai, H., and Manabe, A., "Large-eddy simulation of unsteady flow in a mixed-flow pump" *International Journal of Rotating Machinery*, 2003, volume 9, pp 345–351.

14. Nursen, E. C., and Ayder, E., "Numerical calculation of the three- dimensional swirling flow inside the centrifugal pump volutes" *International Journal of Rotating Machinery*, 2003, volume 9, 247–253.

15. 15 Baun, D. O. and Flack, R. D., (2003), "Effects of volute design and number of impeller blades on lateral impeller forces and hydraulic performance" International Journal of Rotating Machinery, volume 9, pp 145–152.

16. Zhou, W., Zhao, Z., Lee, T. S., and Winoto, S. H., (2003), "Investigation of flow through centrifugal pump impellers using computational fluid dynamics" *International Journal of Rotating Machinery*, volume 9, pp 49–61.

17. Kato, C., Mukai, H., and Manabe, A., (2003), "Large-eddy simulation of unsteady flow in a mixed-flow pump" *International Journal of Rotating Machinery*, volume 9, pp 345–351.

14. Nursen, E. C., and Ayder, E., (2003), "Numerical calculation of the threedimensional swirling flow inside the centrifugal pump volutes" *International Journal of Rotating Machinery*, volume 9, 247–253.

18. Kochevsky1, A. N., Nenya, V. G., (2004), "Contemporary approach for simulation and computation of fluid flows in centrifugal hydromachines*" International Journal of Physics,* volume 36, pp 167-186.

19. J R.Kadambi, Charoennga, Courtwright R,"Investigation of Particle Velocities in a Slurry pump using PIV:Part 1,The Tongue and Adjacent Channel Flow" *Journal Of Energy Resources Technology*, ASME. December 2004, Vol-126/271.

20. Hergt, P., Meschkat, S. and Stoffel, B., "The flow and head distribution within the volute of a centrifugal pump in comparison with the characteristics of the impeller without casing" *Journal of Computational and Applied Mechanics*, 2004, Volume 5, pp 275-285.

21. J.H Horlock. J.D. Denton., A review of some early design practice using computational fluid dynamics and current prospective, *Journal of ASME,* vol 127, 2005

22. Robert Ray., frank Kenyrey., Numerical modelization of the flow in centrifugal pump, *Journal of rotator machinery*, vol 3, 2005, 244-255.

23. Asuaje.F., 2005, "Numerical Modelization of Flow in Centrifugal Pump: Volute Influences in Velocity and Pressure Field", *Internal Journal of Rotator Machinery*, pp 244-255.

24. Yang, C., Min-Guan, K., Dong, C., Liu, D. and Dong, X., 2007, "Analysis of Turbulent Flow in the Impeller of a Chemical Pump", *Journal of Engineering Science and Technology*, Volume: 3, pp 245-258.

25. Cheah, K.W., Lee, T. S., Winoto, S. H. and Zhao, Z.M., 2007, "Numerical Flow Simulation in a Centrifugal Pump at Design and Off-Design Conditions", *International Journal of Rotating Machinery*, Volume 200.

26. Roudnev, A., and Kosmiciki, R.,2007, "Effects of CFD Modeling Configuration on Centrifugal Slurry Pump Casing Wear Prediction", Hydrotransport 17. The 17th *International Conference on the Hydraulic Transport of Solids*, BHR Group.

27. R. Spence, J. Amarla. Teixeira, Incestigation into pressure pulsation in centrifugal pump using numerical method sported by industrial test, *Journal of Computer and fluid*, 2007

28. J.Feng., Hans. Josef. Dohmen., Numercial investigation on pressure fluctuation for different configuration of vaned diffuser pump, *Journal of Rotating machinery*, 2007.

29. Hofmann, M., Stoffel, B., Coutier-Delgosha, O., Fortes-Patella, R., Reboud, J. L., (2007), "Experimental and numerical studies on a centrifugal pump with 2dcurved blades in cavitating condition" *CAV 2001 california institute of technology* pasadena, california, usa 20-23 june, 2001.

30. Younsi, M., Kergourlay, G., Bakir, F., and Rey, R., (2007), "Influence of splitter blades on the flow field of a centrifugal pump: test-analysis comparison" *International Journal of Rotating Machinery*, Volume 07, Article ID 85024, 13 pages.

31. John S. Anagnostopoulos, A fast numerical method for flow analysis and blade design in centrifugal pump impeller, *Journal of computer and fluid*, 2008, pp 284-289

32. M. Pathak, Computational investigation of particulate slurry flow around a square shaped obstruction in a rectangular duct, *Journal of Heat and mass transfer*, 2009

33. Kalekudithi ekambara, R. Sean Sanders, hydraulic simulation of horizontal slurry pipeline using ansys CFX, *Journal of American Chemical Society*, Vol XXX, 2009.

34. Ekambara,K. Sean Sanders, R., Nandakumar, K. and Masliyah J. H., 2009, "Hydrodynamic Simulation of Horizontal Slurry Pipeline Flow Using ANSYS-CFX" *American Chemical Society*

35. Behrouz, J., Hajari, A. and Mehdi M., 2010, "The Flow Simulation of a Low- Specific-Speed, High- Speed Centrifugal Pump" *Applied Mathematics and Modeling* , Eliever publication